1.Reply to the Editor's comments further review by editor and referees(a point-by-point reply to the comments)

Editor Decision: Publish subject to revisions (further review by editor and referees) (15 Nov 2018) by Frederiek Sperna Weiland

Comments to the Author:

The manuscript addresses a relevant topic and especially for this Special Issue the model improvement with satellite data is very valuable. Yet, as also stated by the reviewers, the manuscript needs further improvement. Please address all improvements addressed in your response to the reviewers and pay specific attention to hte following:

1. Improve the English

2. Clearly address the novelty of the research and make sure you link this to other international research and model developments on this topic. The fact that your model has been improved with the specific properties and has been applied for the basin for the first time does not say that it is scientifically novel. Pay more attention to the discussion of the differences, advantages and similarities of your model from the models referenced in the Introduction.

3. Address the model and parameter uncertainty, see the comments of reviewer 2 and pay specific attention to the model calibration and please increase the number of flood events considered. Look for a way to present the relevant statistics efficiently.

4. Make sure the presentation and discussion of results is in the right order.

5. Consider presenting results of the model performance for one of the upstream sub-basins where the influence of Karst highly dominates the runoff processes.

First, thank you very much for the further review by the editor and referees. Below are the individual responses to the editor's and reviewers' comments.

Comment 1.

Improve the English

ACs 1.

The language of the manuscript was improved during the revision process. There were some syntax errors and unclear sentences in the paper. After the editor and reviewer commented on the language of the manuscript, the authors checked the entire paper carefully to correct the language errors. Additionally, we asked

AMERICAN JOURNAL EXPERTS (AJE) for help and chose the "Premium editing package" for revision of the whole paper. Afterward, the authors again reviewed the entire paper carefully to ensure that the language was addressed and that the edits suggested by AJE accurately reflected the meaning of the article.

Comment 2.

Clearly address the novelty of the research and make sure you link this to other international research and model developments on this topic. The fact that your model has been improved with the specific properties and has been applied for the basin for the first time does not say that it is scientifically novel. Pay more attention to the discussion of the differences, advantages and similarities of your model from the models referenced in the Introduction.

ACs 2.

This was completed in the revision. The reviewer pointed out that the novelty of the research is not clear in the original paper. The novelty of this study is described more clearly in the abstract and the introduction in the revision.

The main novelty of the paper is the improvements to the structure and function of the physically based distributed hydrological model, the Liuxihe model, by adding a karst mechanism. For instance, the sub-basins are divided into many karst hydrology response units (KHRUs) in this paper to ensure that the model structure is refined enough to suit karst landforms. In addition, the karst hydrological processes including 'rapid fissure' and 'slow fissure' in the epikarst zone are considered in the model structure.

There is lack of typical rainfall data upon which to build a hydrological model in karst basins, and the PERSIANN CCS QPEs could offer reasonable and high-resolution rainfall data. Coupling the PERSIANN CCS QPEs with a physically based distributed hydrological model has far-reaching application potential in karst flood simulation and prediction. Additionally, recalibrating the coupling model parameters is a novelty of this study, and it can largely improve the flood prediction performance of the model.

The editor pointed out the authors should pay more attention to the discussion of the differences, advantages and similarities of the model in this study from the models referenced in the Introduction. and make sure the model used in this paper is innovative compared with other international research and model developments.

This was completed in the revision. Some of the features and functions unique to the model structure in this paper have been added and described in the introduction. For instance, the early warning points are set up in the model to predict the flood processes of some special points in the river section, for example, at the mouth of the river or at the outlet of the basin. These points have special significance, such as in flood warnings and to ensure safe evacuations. Flood process predictions could be performed separately at these points, and people may pay more attention to these flood processes, which is greatly needed in karst areas.

Comment 3.

Address the model and parameter uncertainty, see the comments of reviewer 2 and pay specific attention to the model calibration and please increase the number of flood events considered. Look for a way to present the relevant statistics efficiently.

ACs 3.

This was completed in the revision. The model parameter uncertainty was analysed and added to section 5.3, Parametric uncertainty analysis, in the revised manuscript. The multi-parameter sensitivity analysis (MPSA) method by Choi (1999) et al. was used to analyse the parameter uncertainty in the model, and it was developed based on the GLUE method.

There are only 5 karst flood events in the original paper, and according to the comments of reviewer, this amount is not sufficient for such a complex model. Therefore, in the revision, 30 karst flood events from 1982-2013 were collected, and 3 were used for parameter optimization, while the others were used to validate the performance of the model. A set of 6 evaluation indices, namely, the Nash-Sutcliffe coefficient, correlation coefficient, process relative error, peak flow relative error, coefficient of water balance, and peak flow time error, are used to present the simulated flood results efficiently.

Comment 4.

Make sure the presentation and discussion of results is in the right order.

ACs 4.

This was corrected during the revision process. The structure of the paper has been modified in the revised manuscript. The original paper structure was as follows: 1 Introduction, 2 Methodology, 3 Study area and data, 4 PERSIANN-CCS QPEs and its post-processed results, 5 Model set up, 6 Results and discussions, and 7 Conclusion.

In consideration of the content in part 4, PERSIANN-CCS QPEs, and part 5, Model set up, we felt that some of this content belonged in part 2, Methodology, so the structure of the paper was modified so that the sequence and the logical relationship were easier to understand. The new structure of the paper is as follows: 1 Introduction, 2 Study area and data, 3 PERSIANN-CCS QPEs, 4 Hydrological model, 5 Model set up, 6 Results and discussion, and 7 Conclusion.

Furthermore, as noted, some of the results were already presented in section 5, before section 6 ‘Results and discussion’. These results were added to section 6 ‘Results and discussion’ during the revision process.

After these revisions, the presentation and discussion of our results now appear in the correct order.

Comment 5.

Consider presenting results of the model performance for one of the upstream sub-basins where the influence of Karst highly dominates the runoff processes.

ACs 5.

This is a valuable suggestion, and it was implemented during the revision. The most developed karst area of the study area, the LKRB, is the Beijiang catchment, where the influence of karst features highly dominates the rainfall runoff processes. The Beijiang catchment is a tributary of the middle and upper reaches of the Liujiang River. The karst floods are typical flash floods with rapid discharge and water level fluctuation in the catchment and are mainly caused by storms, and the developed karst landforms play important roles in flood propagation. For instance, karst depressions can store some water content during the heavy rain. Additionally, the regulation functions of the karst fissure system can slow the flood propagation velocity.

The early warning point at the Goutan river gauge was set in the model to simulate and predict the karst flood process in the Beijiang catchment, since the Goutan point is the outlet of the catchment. In total, 10 karst flood events were collected to validate the flood simulation effect based on the Liuxihe model in the revised manuscript.

References: Choi, J., Harvey, J. W., and Conklin, M. H.: Use of multi-parameter sensitivity analysis to determine relative importance of factors influencing natural attenuation of mining contaminants. the Toxic Substances Hydrology Program Meeting, Charleston ,south Carolina: 1999.

2. A list of all relevant changes made in the manuscript

2.1 Improve the English

The language of the manuscript was improved during the revision process. Some syntax errors, unclear sentences and the language errors in the paper were corrected carefully. And we asked AMERICAN JOURNAL EXPERTS (AJE) for help and chose the “Premium editing package” for revision of the whole paper.

2.2 Clearly address the novelty of this study

The main novelty of the paper is the improvements to the structure and function of the physically based distributed hydrological model, the Liuxihe model, by adding a karst mechanism. The novelty of this study is described more clearly in the abstract (Line 28-38), the introduction (line 94-124, and 185-200) and section 4.2 (line 486-510) in the revision.

And compared with other international research and model developments, the feature and function unique to the model structure in this paper have been added and described in the introduction section. For instance, the early warning points are proposed and introduced in the introduction (line 109-118) and set up in the model to predict the flood processes in section 2.3, line 289-299, section 5.1, line 609-617, and shows in Figure 1.

2.3 Improve the structure of the paper

The structure of the paper has been modified in the revised manuscript. The original paper structure was as follows: 1 Introduction, 2 Methodology, 3 Study area and data, 4 PERSIANN-CCS QPEs and its post-processed results, 5 Model set up, 6 Results and discussions, and 7 Conclusion.

To easier understand the sequence and the logical relationship of the paper, the structure of the paper was modified as follows: 1 Introduction, 2 Study area and data, 3 PERSIANN-CCS QPEs, 4 Hydrological model, 5 Model set up, 6 Results and discussion, and 7 Conclusion.

And some of the results presented in section 5 were added to section 6 ‘Results and discussion’ during the revision process.

After these revisions, the presentation and discussion of our results now appear in the correct order.

2.4 Improve words and sentences

Some words in the paper are modified in the revised manuscript. For instance, the word ‘forecasting’ is mentioned many times in the manuscript, even in the tile, but it is replaced by ‘prediction’ in the whole paper in the revision.

And in section 4.2, equation (4), line 510-513, (original in line 255-258), there is a mistake in spelling, and the word ‘rapid fissure flow’ is changed to ‘slow fissure flow’ in the revision.

In section 4.2, equation (5), line 518-523, (original in line 263-267), ‘the epikarst zone’ is replaced by ‘the slow fissure flow’.

It is not clear how the sub-basins are identified in the study area. The description of the sub-basins is modified in section 4.1, line 432-437, (original in line 192-195): “and the whole catchment is divided into a great number of grid cells horizontally using the high-resolution DEM data, with the divisions called sub-basins. Each grid is considered a uniform basin, and the elevation, land cover type, soil type, and other model elements including rainfall-runoff, evapotranspiration, etc. are calculated in the uniform basin.”

In section 4.2, line 497-510, (original in line 250-256): the paragraph has been rewritten to make the karst hydrological process of the rapid fissure flow and slow fissure flow in the epikarst zone more clear.

In section 4.2, line 524-525, (original in line 268-269): the sentence “The linear reservoir model is employed to calculate the regulation process of the superficial karst fissure system” is replaced by “The linear reservoir model is employed to calculate the regulation process of the superficial karst fissure system in the epikarst zone”

2.5 Add descriptive content and calculation results

In section 1. Introduction, line 109-118, the descriptive content about the early warning points in the model is added.

The distributed hydrological karst models have a direct relationship with the karst landform or geology. However, there is no introduction about the landform or geology in the original paper. In the revised manuscript, section 2.2 Landform, tectonics and hydrogeology information are added (line 236-275).

In section 2.1, line 227-235, the Beijiang catchment is introduced, it is the most developed karst area in LKRB, where the influence of karst features highly dominates the rainfall-runoff processes, and in section 2.3, the early warning point of the Beijiang catchment and the karst flood events are added.

In section 4.2, line 486-510, some key issues are more clearly explained in the model description. For example, the meaning of ‘rapid fissure’ and ‘slow fissure’ in the epikarst zone, the karst hydrological process for rainfall-runoff during the heavy rain, and the hydrological function of the sinkholes.

The karst flood simulation results of Beijiang catchment are calculated in section 6.2 in the revised manuscript (line 768-793). There are 10 karst flood events are simulated in the Beijiang catchment, and the evaluation indices of the simulated flood results are shown in Table 6, and 4 karst flood simulation results are shown in Figure 13.

2.6 Address the hydrogeology parameters and parameter uncertainty

The hydrogeology parameters of the model are added in section 5.2, line 624-651, (original in line 486-495), and listed in Table 2 (b), (c) in the revised manuscript.

The model parameter uncertainty was analysed and added in section 5.3, line 685-711, section 6.1, line 732-754, and in the section 7. Conclusion, line 930-939 in the revised manuscript. The parameter uncertainty results are shown in Table 4.

There are only 5 karst flood events for LKRB in the original paper, in the revision, 30 karst flood events from 1982-2013 were collected in section 2.3, line 278, and 3 were used for parameter optimization in section 5.2, line 660-674. The flood simulation results obtained through parameter optimization by the improved PSO algorithm are shown in Figure 11 and Table 3. The 30 karst flood events simulated results are analysed in section 6.2, line 757-767, and the evaluation indices of the simulated flood results are listed in Table 5.

2.7 The down-scaling method of the PERSIANN data

How the PERSIANN data down-scaling carried out in the original paper is not clear, and in the revised manuscript, section 3.1, line 336-339, add a sentence: the down-scaling method is used in this paper based on statistical relations between meteorological variables, and DEM data using LOO (Leave-One-Out) cross evaluation method and spatial autocorrelation analysis methods (Fan et al., 2017).

2.8 Improve Figures and Tables

Figures:

1) Figures 1 is redrawn, and add Figures 1(b) and (c).

2)The scale of the Figure 2(a)and(b) are modified to the same scale in the revised manuscript.

3) Figures 3,10 are redrawn to make the resolution higher.

4) In Figures 4-8, (original Figure 5-9), there is a mistake for the different colors of the lines. In the revised manuscript, the same colors of the lines and the same range on the x and y axes for the figures are used. And the units of the x axes for the rainfall are converted into mm/hr.

5) Figure 9,11, and 13 are added.

Tables:

1) In Table 1, the Average precipitation and Relative bias are recalculated.
2) In Table 2, (b) and (c) are added.
3) Table 3,4,5 and 6 are added.
4) In Table 7 and 8, the titles are replaced.

To make the descriptions of Table 7 and 8 more clear (original Table 3 and 4), the title of them are modified. Table 7. Evaluation indices of simulated flood events using the initial PERSIANN-CCS QPEs and the post-processed values; Table 8. The effect of recalibrating the coupling model parameters. Also, the flood simulation result by rain gauge precipitation are deleted in Table 8(original Table 4). Because it is not necessary and already exist in Table 7(original Table 3).

In Table 7 and 8, the Peak flow time errors are considerably high. So the coupling model are re-examined and the Peak flow time errors are recalculate in Table 7 and 8. After that, the Errors in time to peak are acceptable.

2.9 Improve References

1) Delete or replace references:

There are two redundant references in this paper:

Original Line189, Chen et al. (2011) in is mentioned in the text but not in the list;

Original Line 964-966, Liang (1997) is in the list, but not mentioned in the text.

Both of them are deleted in the revised manuscript.

Some of the references used in this study are outdated. For instance, Davis (1912), Original line335; Strahler method (Strahler, 1957), line Original 453, and Saxton (Saxton et al.,1986), Original line 485. In the revised manuscript, the references Davis (1912), Strahler method (Strahler, 1957) are deleted, and Saxton (Saxton et al.,1986) is replaced by Ren (2006), line 653.

2) Add references:

Line 560, Ahilan, S., O'Sullivan, J. J., and Bruen, M.: Influences on flood frequency distribution in Irish catchments. 34th IAHR World Congress 2011: Balance and Uncertainty: Water in a Changing World. International Assn for Hydro-Environment Engineering and Research, 2012.

Line 689, Choi, J., Harvey, J. W., and Conklin, M. H.: Use of multi-parameter sensitivity analysis to determine relative importance of factors influencing natural attenuation of mining contaminants. the Toxic Substances Hydrology Program Meeting, Charleston ,south Carolina: 1999 .

Line 338, Fan, K.K.,Duan, L.M.,Zhang, Q., Shi, P.J., Liu, J.Y., Gu, X.H., and Kong, D.D.: Downscaling Analysis of TRMM Precipitation Based on Multiple High-resolution Satellite Data in the Inner Mongolia, China. Scientia Geographica Sinica, 37(9):1411-1421, 2017.

3. A marked-up manuscript version

~~Flood prediction~~Predicting floods in a large karst river basin by coupling PERSIANN-~~-~~CCS QPEs with a physically based distributed hydrological model

Ji Li[1]*, Daoxian Yuan[1,2], Jiao Liu[3],Yongjun Jiang[1], Yangbo Chen[4], Kuo Lin Hsu[5], Soroosh Sorooshian[5]

1. School of Geographical Sciences of Southwest University, Chongqing Key Laboratory of Karst Environment, Chongqing, 400715,China
2. Karst Dynamic Laboratory , Ministry of Land and Resources , Guilin 541004 , China
3. Chongqing Hydrology and Water Resources Bureau, Chongqing, 401120 ,China

4. Department of Water Resources and Environment, Sun Yat-sen University, Guangzhou 510275, China

5. Center for Hydrometeorology and Remote Sensing, Department of Civil and Environmental Engineering, University of California, Irvine
Irvine, California

*Correspondence: Ji Li (445776649@qq.com)

Abstract~~.~~

In general, there are~~There is~~ no long-term meteorological or hydrological data ~~in~~ available for karst river basins~~to a large extent~~. ~~Especially~~The lack of ~~typical~~ rainfall data is a great challenge ~~to build~~theat hinders the development of ~~-a~~ hydrological models. Quantitative precipitation estimates (QPEs) based on ~~the~~ weather satellites ~~could~~ offers a ~~good attempt~~potential method by which ~~to obtain the~~ rainfall data in karst ~~area. What's more~~areas could be obtained. Furthermore, coupling QPEs with a distributed hydrological model has the potential to improve the precision ~~for~~ of flood predictions in large karst ~~watershed~~watersheds. Estimating ~~P~~precipitation ~~estimation~~ from remotely sensed information using an artificial neural network~~s~~-cloud classification system (PERSIANN-CCS) ~~as~~ is a type of QPE technology ~~of QPEs~~ based on satellites that has ~~been~~ achieved ~~a wide~~ broad research results ~~in the world~~worldwide. However, only a few studies on PERSIANN-CCS QPEs ~~are~~ have occurred in large karst basins, and the accuracy is ~~always~~ generally poor in terms of practical ~~application~~applications. This paper studied the feasibility of coupling a fully physically-based distributed hydrological model~~-~~, i.e., the Liuxihe model, with ~~the~~ PERSIANN-CCS QPEs for predicting floods ~~prediction~~ in a large river basin, i.e., the~~-~~ Liujiang K~~k~~arst ~~r~~River ~~b~~Basin, which has ~~with~~ a watershed~~n~~ area of 58,270 km^2~~-~~, ~~watershed~~ in southern China. This study is also the first ~~time that~~to use the Liuxihe model ~~has been used in~~for flood simulations and predictions in karst ~~basin~~basins ~~as an attempt in this study~~. ~~And the~~The model structure and function ~~need to be more~~require further ~~refined~~ refinement to suit the karst basins. For instance, ~~—~~ the sub-basins in

this paper are divided into many karst hydrology ~~respond~~response units (KHRUs) ~~in this paper~~ to ensure that the model structure is adequately refined ~~enough in~~for karst ~~area. What's more~~areas. In addition, the convergence of the underground runoff calculation method within the original Liuxihe model is changed to suit the

karst water-bearing media, and the Muskingum routing method is used in the model to calculate the underground runoff in this study. ~~Also~~Additionally, the epikarst zone, as a distinctive structure of the KHRU, is ~~considered~~ carefully considered in the model. The result of the QPEs ~~result~~ shows that~~,~~ compared with the observed precipitation measured by a rain gauge, the distribution of precipitation predicted by the PERSIANN-CCS QPEs ~~has a great similarity~~was very similar. ~~But~~However, the quantity ~~values~~ of precipitation predicted by the PERSIANN-CCS QPEs ~~are~~ was smaller. A post-process~~ed~~ing method is proposed to revise the products of the PERSIANN-CCS QPEs ~~products~~. The karst flood simulation results show that coupling the post-processed PERSIANN-CCS QPEs with the Liuxihe model has a better performance ~~than~~ relative to ~~the~~ the result ~~with~~ based on the initial PERSIANN-CCS QPEs ~~in karst flood simulation~~. ~~What's more~~Moreover, the performance of the coupled model~~coupling model's performance~~ largely improves ~~largely~~ with parameter re~~-optimized~~ optimization ~~with~~ via the post-processed PERSIANN-CCS QPEs. The average values of the six evaluation indices change as follows: ~~including~~ the Nash–Sutcliffe coefficient ~~has~~ ~~a~~increases by 14% ~~increase~~, the correlation coefficient ~~has a~~increases by ~~14~~15% ~~increase~~, the process relative error decreases by ~~has a~~ 8% ~~decrease~~, the peak flow relative error decreases by~~has a~~ 18% ~~decrease~~, the water balance coefficient increases by~~has a~~ ~~7~~8% ~~increase~~, and the peak flow time error ~~has~~ displays a ~~2~~55 ~~hours~~ -hour decrease~~, respectively~~. Among ~~them~~these parameters, the peak flow relative error shows~~and the peak flow time error have~~ ~~has~~ the ~~biggest~~ greatest improvement~~s~~; thus, these parameters are of the greatest concern ~~which are the greatest concerned factors in~~for flood prediction. The rational flood simulation results ~~by~~from the ~~coupling~~ coupled model provide a great practical application prospect for flood prediction in large karst river basins.

1 Introduction

The highly anisotropic karst water-bearing media and intricate hydraulic conditions ~~make~~ cause ~~the~~ karst flood processes to exhibit significant differences in time and space, which ~~led~~leads to ~~the~~ laminar flow and turbulent flow transmutation~~transmutetransmuting into each other~~ in karst areas; thus, ~~and the~~ flood events in karst river basins are more complicated ~~compared with~~than ~~that of~~ those in non-karst ~~area~~areas (Ford and Williams,2007;Goldscheider and Drew,~~2007）.~~2007). This difference makes it difficult to precisely simulate and forecast the karst flood process ~~based on~~using a hydrological model ~~in mechanism~~. It is ~~a~~ common practice ~~that~~ to simplify ~~the~~ karst water-bearing media ~~should be simplified~~ before ~~build~~building a model. For example, ~~making~~ the karst river basin could be made into ~~as~~ a multiple and nested spatial structure~~;~~, ~~making~~ the underground river ~~as the~~ could be made into an intelligible river system in the model~~;~~, and the cave ~~as~~ could be ~~the~~ an anisotropic medium with a large vertical infiltration coefficient and porosity but a small specific yield. Even so, it is still hard to quantify the spatial structure of ~~the~~ karst water-bearing media with a physics-mathematics model. ~~And the karst~~ Karst flood simulation results usually have some errors that ~~could not~~ cannot be ignored, ~~which is~~and these errors represent the main problem in flood prediction in karst river ~~basins（Kovacs~~basins (Kovacs and Perrochet,~~2011）.~~ 2011).

Because the dynamic changes ~~of~~ in ~~the~~ karst hydrological ~~process~~processes and the hydraulic conditions of the underlying surface are complicated and non-linear in karst ~~area, which makes it hard~~areas, ~~it is difficult to obtain~~ obtaining ~~the hydrogeology~~ hydrogeological parameters, such as specific yield, hydraulic conductivity and aquifer transmissivity, is difficult ~~and so on~~. With the rapid development of remote sensing, GIS technology and hydrogeology, the technology ~~of~~ used in field work, including ~~the~~ tracer tests (Birk et al.,2005;Doummar et al.,2012) and infiltration tests ~~have~~, has made ~~a~~ significant progress. However, ~~it is still a challenge to accurately simulate~~ accurately simulating the laws of motion of ~~the~~ karst hydrological processes in ~~the~~ karst water-bearing media ~~with~~ based on these experimental tests remains difficult. ~~So the~~ Therefore, traditional methods, such as lumped hydrological models, are not suitable for flood prediction in karst ~~area (Hartmann~~ areas (Hartmann et al., ~~2013)~~ 2013). Compared with the performance of lumped hydrological models, ~~the~~ physically based distributed hydrological models (PBDHMs) have some advantages ~~for~~ in terms of generating karst flood predictions ~~in mechanism~~. ~~The~~ PBDHMs divide the ~~whole~~entire karst river basin into a series of small grid units named karst sub-streams, which ~~could~~ precisely reflect the real rules of hydrological processes and karst development characteristics ~~precisely~~. Therefore, ~~it~~ the PBDHM approach has ~~a~~ great application potential ~~to improve~~in terms of improving ~~the~~ karst ~~floods~~flood simulation and prediction ~~capability~~ capabilities (Ambroise et al., 1996). Many PBDHMs have been proposed since the blueprint of the ~~PBDHMs~~ PBDHM was published by Freeze and Harlan (1969). The first full PBDHM ~~is~~, called the SHE model, ~~was regarded as the SHE model and~~ was published in 1987 (Abbott et al., 1986a, b). Shustert and White (1971) attempted to use~~d the~~ the PBDHM ~~as an attempt~~ in karst ~~area, in~~areas. In their research, the dissolved carbonate species were ~~analyzed~~analysed in the waters of 14 carbonate springs in the ~~Central~~ central Appalachians. ~~And these~~ These springs were classified into diffuse-flow feeder-system types and conduit feeder-system types. ~~The~~ PBDHMs have ~~been achieved~~ obtained ~~many~~ several good research results in karst ~~area~~areas (Atkinson,1977; Quinlan and Ewers,1985; Quinlan et al.,2011; Duan and Miller,1997; Ren,2006; Liu et al.,2013; Zhang et al.,2007).

The PBDHM used in this paper is the Liuxihe model ~~(~~ (Chen,2009) ~~)~~, ~~it~~which is a fully distributed model with 14 physically-based parameters. ~~And after~~ After ~~adding~~ the karst mechanisms were added, the number of ~~the~~ parameters ~~is~~ was 20. Unlike other distributed hydrological models, there are some special structural designs in ~~the~~ this model. For instance, the whole model structure is divided into eight independent parts, which are called sub-models~~;~~. ~~t~~These sub-models ~~that~~ ~~including~~include the 1) ~~Watershed~~ watershed division and data mining sub-model, 2) ~~Units~~~~U~~unit classification and river section estimation sub-model, 3) ~~Rainfall~~ rainfall fusion computational~~merged calculation~~ sub-model, 4) ~~Evapotranspiration~~ evapotranspiration calculation sub-model, 5) ~~Runoff~~ runoff calculation sub-model, 6) ~~Confluence~~ confluence calculation sub-model, 7) ~~Parametric~~ parametric sensitivity analysis sub-model, and 8) ~~Parameter~~ parameter optimization sub-model. ~~, among them, u~~Unlike other distributed models, separate parameter uncertainty analysis calculations ~~need to~~must be performed outside the model. However, the parametric sensitivity analysis is a fixed module in the Liuxihe model, which means that when the model is built for flood prediction, parametric uncertainty analysis has already been carried out. ~~And the~~The parametric uncertainty analysis

in the Liuxihe model is based on a ~~Multi~~multi-~~Parameter~~ parameter ~~Sensitivity~~ sensitivity ~~Analysis~~ analysis that was presented by ~~by in~~ Choi (1999) et al.

In ~~the~~ actual flood predictions, people may pay more attention to the flood process ~~of~~ at ~~some special~~specific points ~~on~~ of the river section. For example, focus may be directed at~~on~~ the mouth of the river or the outlet of the basin. ~~And these~~ These points have special significance in relation to procedures such~~, such~~ as flood warnings and ~~getting, get evacuees to safety~~evacuations~~safely, etc~~. Therefore, ~~it is very important to extract~~ extracting the flood processes ~~of~~ at these points is important and should be given~~and make a special display give them~~ special consideration.~~—~~ In the Liuxihe model, these points are named early warning points, and flood prediction, which is ~~badly~~urgently needed in karst areas, can be ~~done~~performed separately at these points~~, which is badly needed in karst areas~~.

For ~~instance~~example, the ~~confluent~~confluence of ~~the~~ underground rivers could be established through a field survey and a geological borehole test and set ~~to become~~as ~~a~~an early warning point ~~through the field survey, and geological borehole test, -~~ because this is a point ~~where~~ at which the influence of karst ~~highly~~ may dominate the runoff processes.

In addition, the catchment property data for the Liuxihe model, which primarily include the~~mainly including~~ digital elevation model (DEM), land use and soil types, can be easily downloaded from ~~the~~ open-access databases for free. ~~This means~~Therefore, ~~you can easily build~~ the Liuxihe model ~~in your area~~can be built in any area. ~~Considering that~~Though it is not easy to obtain the basic data needed to build~~for building~~ a distributed hydrological model in karst areas, ~~but 2~~only a very small amount of data must be~~need to~~ downloaded from the web to build the Liuxihe model, making it ~~is~~ a feasible option for flood simulation and prediction in karst basins.

~~Since the~~ The regulation and storage capacity of ~~the~~ karst water-bearing media are weak. When the accumulated rainfall exceeds the maximum drainage capacity of the channel during a heavy rain storm, a~~then the~~ karst immersion-waterlogging hazard is much more likely to ~~appear in this situation~~occur. ~~And the~~ The hazard will become ~~more and more~~ increasingly serious with the intensification of extreme global ~~extreme~~ weather events. ~~So~~Therefore, some effective measures need to be taken to reduce ~~the~~ losses caused by floods~~ losses~~. For example, effectively and reliably simulating and ~~prediction~~predicting the karst flood process using ~~reliably with~~ a PBDHM~~ effectively, it is~~ is an important non-project measure for flood control. However, there ~~is no enough~~are insufficient rain gauges ~~as well as the~~ and long-term meteorological or hydrogeological data available to build a PBDHM in karst river basins~~ where is~~ classified as ~~an belongs to~~ ungauged basins. Predictions in ungauged basins (PUB) ~~is~~ are the theme of the international hydrological decade,~~;~~ at the core of which is runoff calculation (Li and Ren, 2009). Therefore, it is more difficult to forecast ~~the~~ flood events in karst river ~~basin compared with that of~~ basins than in non-karst ~~area~~areas. How to solve the problem of rainfall ~~source~~sources is a key factor ~~of~~in the current karst flood prediction challenge. ~~The quantitative~~ Quantitative precipitation estimates ~~(~~(QPEs)~~,~~ ~~especially~~ and, particularly, ~~the~~ satellite ~~QPEs~~QPE technology~~ brings the possibility,~~ make it possible to obtain ~~the~~ reasonable rainfall data in karst ~~area. But~~areas. However, the current application of ~~the~~ QPEs is ~~not mature enough~~immature, which ~~makes~~ results in ~~the~~ poor QPE accuracy~~, of the QPEs as well as~~ and the effect of the karst flood simulation and prediction ~~to being poor~~is also poor~~are not so good~~.

The ~~developed~~ development of numerical weather prediction models in ~~the past decades~~recent decades has provided a reasonable and accurate ~~QPEs~~QPE product that can be used in karst ~~area~~areas. The current mainstream QPEs ~~including~~include ~~the~~ weather radar QPEs (Delrieu et al.,2014; Rafieei et al.,2014; Faure et al.,2015), satellite QPEs and ~~radar~~ radar-merging satellite QPEs (Stenz, 2014; Bartsotas et al.,2017; Goudenhoofdt and Delobbe,2009; Wardhana et al.,2017~~), —~~). Additionally, ~~P~~precipitation can be ~~estimation~~ estimated from remotely sensed information using ~~Artificial~~ artificial ~~Neural~~ neural ~~Networks~~networks/PERSIANN QPEs (Soroosh et al.,2000; Hirpa et al.,2010; Romilly, 2011;Yang et al.,2007), the dPERSIANN-~~Climate~~ climate ~~Data~~ data ~~Record~~record/PERSIANN-CDR (Ashouri et al., 2014; Liu et al., 2017; Tan and Santo,2018; Hussain et al., 2018), and the PERSIANN-~~Cloud~~ cloud ~~Classification~~ classification ~~System~~system/PERSIANN-CCS (Yang et al., 2004,2007; Moradkhani and Meskele, 2010)~~)~~. ~~The research~~ ~~Studies of~~ Studying ~~on~~ the QPE~~s~~ products ~~by~~ from meteorological satellites has become a ~~hotspot~~ popular topic in rainfall prediction research (Hu et al., 2013).

~~Although m~~Many scholars at home and abroad have ~~done a lot of~~performed ~~–~~considerable research ~~with~~ using ~~the QPEs~~QPE technology, and they have ~~also~~ achieved many acceptable ~~accepted~~ results. However, ~~there are~~ considerable uncertainty exists in the application of these results, which ~~makes~~ causes the precision of the QPEs ~~is~~ to be low; thus, ~~and~~ the precipitation result ~~by~~ generated from the QPEs ~~is not satisfactory~~may be unsatisfactory. Two effective measures could reduce the uncertainty of ~~the~~ QPE~~s~~ results in the karst area. One measure is to match the appropriate resolution of the model. ~~Because t~~The resolution can directly affect the results of the QPEs ~~directly.~~; thus, if the resolution is too low, then the division of the grid units ~~divided are~~is too coarse, which causes a considerable error in the rainfall estimates~~;~~. However, if the resolution is too high, then the meteorological model structure is complicated and unstable. Furthermore, the ~~requirement~~ required~~of~~ computational resources will increase exponentially ~~with~~ as the ~~the raise of the~~ model spatial resolution increases (Chen et al., 2017), which leads to ~~huge~~ a large number of calculations and low efficiency. ~~So~~Therefore, using the appropriate model spatial resolution is extremely important ~~for~~ in terms of the QPE results~~ of QPEs.~~. ~~And the~~The other measure that affects uncertainty is that the current technology of QPEs still has some systematic errors ~~existed~~ due to ~~the~~ uncertainties in the structure and mathematical ~~algorithm~~algorithms. For this reason, when compared with the precipitation observed using ~~by the~~ rain gauges, the results of QPEs ~~compared with the observed precipitation by rain gauge~~ have some relative errors, ~~which causes~~and these errors cause the karst flood simulation results ~~by~~ from the ~~coupling~~ coupled model (i.e., those from coupling the QPEs with a PBDHM) to have uncertainties that largely affect the model's performance ~~largely. So~~. Therefore, the results of the initial QPEs could not be directly used ~~directly~~ to build the ~~coupling~~ coupled model. In this study, a post-process~~ed~~ing method ~~is~~ was employed to revise the productions of the PERSIANN-CCS QPEs products, which ~~makes~~ caused the QPE results to be ~~of QPEs~~ more credible and receivable.

There ~~are~~ have been many ~~researches~~studies o~~n~~f PERSIANN-CCS QPEs (Yang et al. 2007)~~ at present~~. ~~But~~However, most of ~~them~~ these studies have been ~~used~~ conducted in small non-karst watersheds. In this study, the PERSIANN-CCS QPEs ~~is~~were employed in an attempt to ~~to~~ estimate the rainfall data ~~as an attempt in such~~in a large karst river basin, i.e., the Liujiang Karst River Basin (LKRB), which has~~with~~ an area of 5.8×~~*~~10^4 km^2 and is located in Guangxi ~~province~~Province, China.

Watershed flood prediction relies on a PBDHM ~~for~~ as a computation tool, while ~~the~~ precipitation is the ~~model's~~ driving force ~~of~~ behind the model (Li et al., 2017). This method~~It~~ has the potential to improve the accuracy of karst flood predictions by coupling PERSIANN-CCS QPEs with a PBDHM. ~~And the~~ The PBDHM in this study is the Liuxihe ~~model（Chen,2009）~~ model (Chen, 2009). This ~~report~~study –is ~~also~~ the first time ~~time that~~ to use the Liuxihe model ~~has been used in~~ for flood simulation and prediction in karst ~~basin~~basins ~~as an attempt~~.
~~So~~Therefore, the model structure and function have been~~are~~ improved to suit the requirements of the karst basin~~s~~. For instance, in this study, the ~~whole~~ entire river basin will be divided into many small sub-basins ~~by~~ using the DEM data ~~in this study~~, and this process is ~~enough~~ adequate when considering~~in~~ non-karst basins. However, ~~in order~~ to ensure the effect and accuracy of the model in karst ~~area~~areas, the model structure ~~needs to~~must be more refined. ~~So~~Thus, in this paper, the sub-basins will be further divided into many karst hydrology ~~respond~~response units (KHRUs) ~~in this paper~~. ~~And the~~ The ~~whole~~ entire karst hydrological process~~es~~, including the storage and regulation processes of the epikarst zone and~~,~~ the spatial interpolation of the precipitation, evapotranspiration and rainfall-runoff, are all calculated ~~on~~ based on the KHRUs. ~~What's more,~~ Furthermore, in the original Liuxihe model, the underground layer is treated as an integral unit, ~~,~~ and a linear reservoir method is adopted to calculate the amount of underground runoff. However, ~~considering that~~because the structure of the karst underground layer is non-linear, the original linear reservoir method ~~in~~ of the Liuxihe model is — not appropriate ~~here~~. ~~So~~Therefore, in this study, the Muskingum routing method is used to improve the convergence of the underground runoff ~~calculation~~calculations ~~in this study~~. ~~Also~~Additionally, the epikarst zone, as a distinctive structure of the KHRU, is carefully considered ~~carefully~~ in the model. An exponential decay equation is used to calculate the regulation and storage processes in the epikarst zone.

The spatial resolution of the Liuxihe model for the LKRB is –200 m×~~*~~200 m. ~~And t~~The ~~the The~~ PERSIANN-CCS ~~QPEs~~QPE products, which have ~~that the~~ a spatial resolution ~~is~~of 0.04°×~~*~~0.04° ~~scale~~ and a time interval ~~is~~of 30 min,~~utes~~ are employed to estimate the precipitation results for the LKRB. The resolution of the PERSIANN-CCS QPEs must be downscaled to the same size as the Liuxihe model before ~~building~~ the ~~coupling~~ coupled model can be built. After post-processing, ~~T~~the PERSIANN-CCS ~~QPEs~~QPE products ~~after post-processed~~ could offer ~~the~~ high-precision precipitation results for the LKRB in locations where there is an inadequate number of ~~lack of enough~~ rain gauges. ~~It can largely improve~~Additionally, ~~the~~ the model performance can be greatly improved by coupling the post-processed PERSIANN-CCS QPEs with the Liuxihe model. A modified PSO algorithm (Chen et al., 2016) is used to optimize the ~~coupling~~ coupled model parameters in this paper, ~~which~~ and this method could control the uncertainty of ~~the~~ parameterization ~~passing~~.

2 Study area and data

2.1 Study area

The ~~Liujiang Karst River Basin (~~LKRB~~)~~ in southern China ~~is~~was selected as the study area ~~in this paper~~for this research. ~~It~~ The LKRB is the second largest tributary of the Pearl River and~~that~~ covers three provinces, including — Guizhou, Guangxi and Hunan ~~province~~. The LKRB is the most developed karst area of China, with a drainage area of 58270 km^2 and a channel length of 1121 km. Moreover, the LKRB is a typical karst-mountainous catchment ~~with~~ that has experienced frequent flash flooding in ~~the~~ past centuries. ~~.~~The peak forest-plain area is the main karst landform on the ground, while the karst conduit and fissure are well -developed underground~~, also there are~~. There are also many complicated underground rivers and springs with large flows (Li, 1996). The karst water-bearing media is highly non-linear and heterogeneous, which makes it very difficult to simulate and forecast the karst hydrological process.

The LKRB is in the sub-tropical monsoon climate zone, with an average annual precipitation ~~of~~between ~~1400mm~~ 1400 mm ~~to~~and ~~1700mm~~ 1700 mm, and the precipitation distribution is highly uneven ~~at~~on spatial and temporal ~~scale~~scales. The precipitation from April to September accounts for 75%~~- to~~ 80% of the annual precipitation. ~~The~~ A sketch map of the LKRB is shown in Figure 1a.

The most developed karst area in LKRB is the Beijiang catchment, where the influence of karst features highly dominates the rainfall-runoff processes. The Beijiang catchment is a tributary of the middle and upper reaches of the Liujiang ~~r~~River, l~~ies~~ying at 25°06-25°27' north latitude and~~,~~ 108°38-109°18' east longitude. The drainage area of the Beijiang catchment is 1790 km^2, and the length is 130 km. The catchment has a dense river system (Figure 1b)~~,~~ and is surrounded by high mountains with peak elevation at 1000–-1800 m (Figure 1c), ~~where~~ in which the peak-cluster depression covers most of the area. The average valley slope gradient is 0.143.

Figure 1. Sketch map of Liujiang and the Beijiang –catchment

2.2 Landform, tectonics and hydrogeology information

The LKRB is located in the central part of Guangxi ~~province~~Province, China. The terrain is high on all sides and low in the middle. The cross-strait terraces of the Liujiang ~~river~~River are well developed~~.~~, especially near ~~by~~ the ~~liuzhou~~ Liuzhou ~~river~~ River gauge (as shown in Figure 3) ~~that~~, which is located at the ~~basin~~ outlet of the LKRB. The north part of the basin ~~is the~~has transmeridional arc-like folded belts, where the soluble rock forms syncline~~,~~ and the sand shale forms anticline. ~~The s~~Sand and shale formations and~~,~~ carbonate and carbonate clastic rocks are widely distributed here. The karst valley is the main landform in the south part of the basin, and– the ~~overburden~~ overlying lithology is clay and gravel with poor water permeability. The underlying bedrock is mainly carbonate and dolomite, ~~where~~ and the karst fissures are well developed~~- developed~~, ~~within a large water storage are well developed~~~~reservoir~~in which a large amount of water is stored (He,2017).

–The western part of the basin has~~is~~ a large area of limestone in a continuous distribution, and ~~the~~ a peak-cluster depression covers most of the area. The landform of the eastern basin is mainly hilly, where the rocks are soft-hard due to ~~the~~their different anti-erosion ~~ability~~abilities. The hard rocks form low mountains that move ~~toward~~ towards the gentle slope~~,~~ ~~but~~ and then back to the steep slope. The landforms of the central part of the basin are mainly the isolated peak plain and the peak forest plain. Overall, the main landforms of the LKRB are the peak forest plain and the peak-cluster depression.

The Liujiang ~~river~~River is located in the karst valley basin, which ~~that~~ is covered by quaternary loose deposits. ~~And the~~ The underlying surface ~~are~~is dominated by ~~the~~ alluvium~~.~~, diluvium and ~~the~~ katatectic layers due to the fluviraption of the ~~liujiang~~ Liujiang ~~r~~River and the karst geological background, ~~where~~ and the thickness is ~~about~~approximately 10-20 ~~meter~~ metres. Carbonate, sandstone, shale and carbonate clastic rocks are widely distributed in the basin~~,~~. ~~a~~Among them, the area of the carbonate rocks is about ~~19230km^2, account~~ 19,230 km^2, which accounts for 33% of the ~~whole~~entire watershed. The outcrops in the basin mainly include ~~the~~ Upper Devonian limestone (D$_3$), ~~the~~ Lower Carboniferous ~~datangpo~~ Datangpo formation limestone (C$_1$d,C1d^3), ~~the~~ Middle (C$_2$d) and Upper Carboniferous (C$_3$) limestone, ~~the~~ Upper Permian carbonate and clastic rocks (P$_2$d, P~~$_2$h~~$_{2h}$), ~~the~~ Lower Triassic clastic and carbonate rocks (T$_1$), ~~the~~ Lower Cretaceous clastic and carbonate rocks, and ~~the~~ loose rock groups of the Quaternary ~~pleistocene~~ Pleistocene (Q,Q$_p$) and Holocene (Q$_h$).

After ~~studied~~studying the karst geomorphology of the LKRB, ~~Williams~~ Williams (1987) believed that the peak-cluster depression had developed into turreted peak-forest landforms after a long evolutionary process, which is equivalent to the late prime of life, i.e., entering old age in terms of~~, and going into the old age of~~ geomorphologic evolution. ~~The allogenic~~ Allogeneic water, especially from the Liujiang ~~river~~River, is the main driving force ~~for~~ behind the development of peak-forest landforms. Therefore, the peak-forest plains and valleys are often distributed in contiguous areas near the main trunk stream of the Liujiang ~~river. And the~~River. The main karst landform of the LKRB is peak-forest plain, and there are also some peak-cluster depressions and peak-forest valleys. Figure 2~~.~~ ~~are~~shows the DEM and three-dimensional topographical map of the LKRB.

Figure 2. The DEM and three-dimensional topographical map of LKRB.

~~Figure~~

2.3 Rain gauges and ~~the~~ karst flood process

There are 68 rain gauges and 131 grid points ~~of~~ for the PERSIANN-CCS QPEs within the LKRB, and data from 5~~five~~ karst flood events that occurred between~~from~~ 2008 ~~to~~ and 2013 were ~~has been~~ collected ~~respectively~~. There ~~is a~~was one flood event each year. The karst floods process in the LKRB ~~have~~ has typical characteristics: the flood peak flows usually exceed 10,000 ~~v~~m^3/s, and there is an expression of ~~the~~ a multi-~~peaks~~peak flood process. A flood process usually lasts ~~about~~approximately 10 days, and the shortest flood event duration ~~is~~ was only ~~about~~approximately 3 days, while the ~~the~~ longest ~~is~~ was 25 days. ~~The h~~Hourly precipitation data ~~of~~ were collected from the rain gauges ~~are collected~~ in this study, and these results were compared with the ~~to compare with the~~ results ~~of~~ from the PERSIANN-CCS QPEs. The rain gauges, the grid points of the PERSIANN-CCS QPEs and the Liuzhou ~~river~~ River gauge that ~~closes~~is located close to the outlet of the LKRB are shown in Figure 1a.

There are 11 early warning points ~~are~~ set in the Beijiang catchment (Figure 1b), and 10 karst flood events at the Goutan warning point ~~are~~ were collected to validate the flood simulation effect based on the Liuxihe model, ~~where~~ in which the Goutan point is the outlet of the Beijiang catchment. In fact, the Beijiang catchment is in the centre of the storm area of Guangxi ~~p~~Province, China.

According to ~~the~~ field observation data, the observed maximum 24-~~-~~hour accumulated precipitation is 779.11 mm in the Beijiang catchment, and the maximum 3-~~-~~day accumulated precipitation is 1335.15 mm. ~~The~~ K~~k~~arst floods are ~~the~~ typical flash floods with rapid discharge and water level fluctuation, ~~which are~~ mainly caused by storms, and the developed karst landform plays an important role in flood propagation. For instance, the karst depressions ~~could~~ can store some water content during ~~the~~ heavy rain. ~~Also,~~Additionally, the regulation functions of the karst fissure system ~~could~~ can slow ~~down~~ the flood propagation process.

~~Figure 3.~~

~~Figure~~

2.4 Property data

The ~~C~~catchment property data for the distributed hydrological ~~model~~models mainly include the DEM, land use and soil types. These data ~~are~~ were downloaded from ~~an~~ open-~~-~~access databases. The DEM ~~is~~ was downloaded from the shuttle radar topography mission database at http://srtm.csi.cgiar.org (Falorni et al., 2005, Sharma et al., 2014). The downloaded DEM ~~has~~ had an initial spatial resolution of ~~90m*90m~~ 90 m×90 m, and after many model resolution tests, the most appropriate resolution ~~for~~ of the Liuxihe model in the LKRB ~~has been~~was confirmed to be ~~as 200m*200m~~200 m×200 m ~~for Liuxihe model in LKRB~~. ~~So~~Therefore, the spatial resolution of the initial DEM ~~is~~ was rescaled to ~~200m*200m~~200 m×200 m in this study, and this value represents~~which is~~ ~~a~~the high resolution for the Liuxihe model in the LKRB. The DEM is shown in Figure 2(a). The land use-~~[-~~type ~~is~~ data were downloaded from http: //landcover.usgs.gov (Loveland et al., 1991, 2000), and the soil-~~-~~type ~~is~~ data were downloaded from http://www.isric.org. The initial spatial resolutions of the land use-~~-~~type and soil-~~-~~type data ~~are~~ were both ~~1000m*1000m~~1000 m×1000 m. However, ~~B~~both ~~of them~~resolutions had ~~need~~ to be rescaled to ~~200m*200m~~200 m×200 m in this study. Figure ~~4~~ 3 (a) ~~is~~shows the land use types, and (b) ~~is~~shows the soil types.

(a) land use types (b) soil types

Figure 3. ~~The p~~Property data for the Liuxihe model in LKRB

~~Figure~~

3 PERSIANN-CCS QPEs and ~~its~~ post-~~processed~~ processing results

3.1 PERSIANN-CCS QPEs

The original PERSIANN system (Hsu et al., 1999) was based on geostationary infrared imagery and was later extended to include the use of both infrared and daytime visible imagery~~;~~. ~~t~~This method represents an~~, which is an~~ automated system for estimating precipitation ~~estimation~~ from remotely sensed information ~~using~~ through the use of artificial neural networks~~.T~~. The ~~system~~ method for rainfall estimation that is under development at ~~The~~ the University of Arizona ~~and gets constantly~~is continuously improving as technology advances~~stronger with the improvement of the technology~~ (Soroosh et al.,2000). The fundamental algorithm of the PERSIANN system is based on a neural network. ~~And the~~The network parameters could be optimized by an adaptive training characteristic, which ~~makes~~ can estimate the precipitation ~~could be estimated~~ from a geosynchronous satellite at any time and place.

The ~~Precipitation Estimation from Remotely Sensed Information using Artificial Neural Networks-Cloud Classification System /~~PERSIANN-CCS (Yang et al., 2004; Hsu et al., 2007)~~—~~ is a patch-based cloud classification and rainfall estimation system from low Earth-orbit~~ing~~ and geostationary satellites ~~by~~ that uses ~~using~~ pattern recognition technology and computer imaging technology (Yang et al.,2007). Satellite-based precipitation retrieval algorithms use information ranging from visible (VIS) to infrared (IR) spectral bands of ~~Geostationary~~ geostationary ~~Earth~~ earth ~~Orbiting~~ orbiting (GEO) satellites and microwave (MW) spectral bands (Hsu et al., 2007).

The ~~QPEs~~QPE products of PERSIANN-CCS ~~has been~~ have generated precipitation estimates at a resolution of 0.04°×~~*~~0.04° scale and at a time interval of 30 min~~utes~~ since 2000. The output of PERSIANN-CCS QPEs ~~has been~~was downscaled at ~~200m*200m as~~ 200 m×200 m to achieve the same spatial resolution as that of the Liuxihe model in the LKRB. ~~And the~~ The down-scaling method ~~is~~ used in this paper was based on statistical relationships between the meteorological variables~~,~~ and DEM data using the LOO (~~Leave~~leave-~~One~~one-~~Out~~out) cross evaluation method and spatial autocorrelation analysis methods (Fan et al., 2017).

The hourly precipitation data ~~of~~ from the PERSIANN-CCS QPEs ~~are~~ were collected and compared with the precipitation observed by the rain gauges.

The ~~R~~estimation of rainfall ~~estimation~~ from the PERSIANN-CCS consists ~~as~~of the ~~follow~~following steps (Hsu, 2007):

(1) IR cloud image segmentation, (2) ~~Characteristic~~ characteristic extraction from IR cloud patches, (3) ~~Patch~~ patch characteristic classification, (4) o~~O~~btaining the rainfall estimation results of ~~QPEs~~the QPE products, and (5) ~~Evaluate~~ evaluating and revising the results of the ~~QPEs~~QPE products.

In this paper, the PERSIANN-CCS QPEs real-time data used in the LKRB from the current version of PERSIANN-CCS are available and downloadable online (http://hydis8.eng.uci.edu/CCS/).

3.2 Precipitation estimation results

The ~~QPEs~~QPE product of the PERSIANN-CCS ~~has been~~ generated precipitation ~~result~~results for the LKRB~~ in this study~~. There ~~are~~ were 131 grid points of PERSIANN-CCS QPEs within the LKRB, ~~which~~and these points were ~~are~~ representative and ~~can~~ completely covered the ~~whole~~entire watershed ~~completely~~ (as shown in Figure 3). The spatial resolution ~~is~~ was

~~200m*200m~~200 m×200 m, and the time interval ~~is~~ was 1 hour. The respective ~~QPEs~~QPE products of the PERSIANN-CCS in 2008, 2009, 2011, 2012 and 2013 ~~are~~ were produced ~~respectively, means there are~~ , and the results indicated that ~~five~~5 rainfall events ~~are corresponding~~ corresponded to the ~~five~~5 karst flood processes. Figures ~~5-9~~4-8 ~~is~~show the average precipitation pattern comparisons of the two precipitation products ~~in~~ of the ~~five~~5 years, ~~and~~where (a) is the average precipitation ~~of~~ based on data from the rain gauges~~,~~;~~—~~ (b) is the average precipitation ~~of~~ based on the data from the PERSIANN-CCS QPEs~~.~~, and (c) is the q~~Q~~uantile-~~Q~~quantile plot, in which the 45-degree line is used to compare two precipitation products.

Figure 4. Precipitation pattern comparison of two precipitation products (2008)

Figure 5. Precipitation pattern comparison of two precipitation products (2009)

Figure 6. Precipitation pattern comparison of two precipitation products (2011)

Figure 7. Precipitation pattern comparison of two precipitation products (2012)

Figure 8. Precipitation pattern comparison of two precipitation products (2013)

~~Figure~~

According to the results of Figures~~—~~ ~~5-9~~4-8, it appears that the temporal average precipitation ~~pattern~~patterns of both products are quite similar, especially in terms of the rainfall distribution, while there are some ~~difference~~differences in the quantitative values.~~—~~ The results ~~of~~ from the PERSIANN-CCS QPEs are smaller than ~~that~~those ~~of~~ from the rain gauges, which means that ~~there is~~ a relative error exists between the two products. From the ~~Q~~quantile-~~Q~~quantile plot, the two rainfall scatter plots are closely distributed on both sides of the 45-degree line, which means that the rainfall distribution of both products ~~is~~ are close to each other.

3.3 Evaluation of PERSIANN-CCS QPEs~~–~~

~~In order to~~

To quantitatively evaluate the results of the PERSIANN-CCS QPEs, the precipitation ~~by~~ from the PERSIANN-CCS QPEs and the precipitation from the rain gauges ~~are~~ were compared in this study. The rainfall distribution of both products ~~are~~is shown in ~~Figs.~~Figures ~~5-9~~4-8. ~~To make~~For further comparisons, the average precipitation of the ~~five~~5 karst flood events ~~are~~was calculated, and the results are shown in Table 1.

Table 1. Precipitation pattern comparison of two precipitation products

~~Table~~

According to the results of Table 1,~~ it could be found that ~~ there are obvious relative errors between the two precipitation products. The average ~~precipitations~~precipitation values of the PERSIANN-CCS QPEs ~~are~~were lower than those from~~ smaller than that of~~ the rain gauges. For the ~~five~~5 karst flood events from 2008 to 2013, the relative errors between the two products ~~are~~ were -~~16~~11%, -~~25~~16%, -~~14~~7%, -~~21~~19% and -~~23~~20%, respectively. The average relative error ~~is~~ was -~~20~~14%, and the maximum error ~~is~~ was -~~25~~20%, which means that these relative errors ~~could~~ cannot be ignored. ~~So~~Therefore, the precipitation results generated by the PERSIANN QPEs must ~~to~~ be revised effectively, and the precipitation data observed by the rain gauges can be~~ are~~ used to revise the results of the PERSIANN QPEs in this study.

3.4 The post-processed PERSIANN-CCS QPEs

~~In order to~~ To make the results of the PERSIANN QPEs more credible and receivable, the precipitation results ~~by PERSIANN QPEs are~~were revised ~~with~~ using the observed precipitation measured by the rain gauges. ~~Firstly~~First, it was necessary to locate~~finding~~ the grid points of the PERSIANN-CCS QPEs that w~~are~~ ere closest to the rain gauges (as shown in Figure 3). ~~And there~~There ~~are~~ were 23 grid points in the LKRB. ~~Secondly~~Second, ~~calculating~~ the~~ir~~ average precipitation values of the PERSIANN-CCS QPEs and the rain gauges were calculated, and the ~~, and taking the~~ average precipitation ~~of~~ from the rain gauges was used as the true precipitation value. ~~Thirdly~~Third, the process of revising the results of the PERSIANN QPEs ~~with~~ based on the average precipitation observed by the rain gauges~~.The procedure~~ is summarized as follows.

1). ~~Calculating the~~The average precipitation of these 23 grid points based on the PERSIANN-CCS QPEs was calculated with the following equation:~~.~~

$$\bar{P}_{PERSIANN-CCS} = \frac{\sum_{i=1}^{N} P_i F_i}{N} \tag{1}$$

~~Where,~~where $\bar{P}_{PERSIANN-CCS}$ is the average precipitation of the~~se~~ 23 grid points ~~by~~ based on the PERSIANN-CCS QPEs,~~;~~ P_i is the precipitation based on the PERSIANN-CCS QPEs ~~on~~ at the i grid point,~~;~~ F_i is the catchment area of the i grid point,~~;~~ and N is the number of ~~the~~ grid points.

2). ~~Calculating the~~ The average precipitation of the~~se~~ 23 rain gauges was calculated using the following equation:~~.~~

$$\overline{P}_2 = \frac{\sum_{j=1}^{M} P_j}{M}$$

~~(~~(2~~)~~)

~~Where,~~where $\overline{P}_2$ is the average precipitation observed by the~~se~~ 23 rain gauges~~;~~, P_j is the precipitation observed at~~by~~ the j rain gauge~~;~~, and M is the number of rain gauges.

3). The precipitation values~~s~~ observed by the adjacent rain gauges ~~are~~ were used to revise the results of the PERSIANN-CCS QPEs with the following equation~~.~~:

$$P_i' = P_i \frac{\overline{P}_2}{\overline{P}_{PERSIANN-CCS}}$$

~~(~~(3)~~)~~

~~Where,~~where P_i' is the value of precipitation based on the PERSIANN-CCS QPEs after ~~revised~~ revision on the i grid point,~~;~~ and $\overline{P}_2 / \overline{P}_{PERSIANN-CCS}$ is the ~~revise~~revised factor.

4). After revision, ~~T~~the precipitation results based on the PERSIANN-CCS QPEs ~~after revised will be~~were used as input data for the Liuxihe model to test its feasibility ~~through the~~ ~~of~~for use in the ~~for floods~~flood simulation.

~~From the~~After running the ~~above procedure of the~~ post-~~processed~~ processing procedure for the PERSIANN-CCS QPEs described above, it ~~could be found~~was determined that the ~~revise~~revised factor $\overline{P}_2 / \overline{P}_{PERSIANN-CCS}$ ~~is~~ was a key factor that made~~to make~~ the results of the PERSIANN-CCS QPEs much closer to the value of observed precipitation recorded by the rain gauges, ~~means~~indicating that the systematic errors of the PERSIANN-CCS QPEs could be corrected effectively. ~~So~~Therefore, the post-~~processed~~ processing method described in this paper is ~~a~~ both feasible and necessary. ~~And it~~ Additionally, it could greatly improve the accuracy of the ~~coupling~~ coupled model in the simulation and prediction of karst floods~~ simulation and prediction~~. Furthermore, the ~~revise~~revised factor could be preserved as an empirical value for ~~the~~ future flood prediction in the LKRB.

4 Hydrological model

4.1 Liuxihe model

The Liuxihe model proposed by Yangbo Chen (Chen, 2009) of Sun Yat-Sen University, China, is employed as the fully distributed hydrological model in this study, which is a physically based distributed hydrological model ~~(~~ (PBDHM ~~)~~) mainly for catchment floods simulation~~g~~ and prediction (Che~~n~~en et al., 2016,2017; Li et al., 2017). The Liuxihe model earned its name by being the first successful application in the Liuxihe catchment, Guangdong P~~p~~rovince, China. There are three layers vertically, including the canopy layer, the soil layer and the underground layer in the model, and the whole catchment is divided into a great number of grid cells horizontally ~~by~~ using the high-resolution DEM data, with the divisions ~~named~~ called sub-basins. Each grid is considered ~~as~~ a uniform basin, and the elevation, land cover type, soil type, and other model elements including rainfall-runoff, evapotranspiration, etc.~~ and so on~~ are calculated ~~on~~ in the uniform basin. All cells are categorized into three types, namely, hill slope cell, river cell and reservoir cell.

An improved PSO algorithm (Chen et al., 2016) is employed to optimize the model parameters in this study, which can make the model's performance much better in flood prediction in karst river basins. The observed meteorological and~~,~~ hydrological data and the development conditions of the karst underground river are used to optimize the model parameters. The terrain property data, ~~like~~such as the DEM, land use type and soil type, can be downloaded freely from an open-access database~~s~~ ~~onling~~online~~ the website~~. The model is validated ~~by~~ against observed karst flood events. ~~All t~~These factors of the model are physically based and rational to truly reflect the underlying surface of the karst basin. ~~So~~ Therefore, this~~it~~ implie~~d~~s that the Liuxihe model could be used for real-time flood prediction in karst river basins. Figure 9~~. is~~shows the structure of the Liuxihe model.

Figure 9. The structure of the Liuxihe model

4.2 ~~The i~~Improvement of the Liuxihe model

The Liuxihe model has been successfully applied ~~successfully~~ for ~~floods~~flood predictions in many river basins. However, ~~all~~ none of these basins ~~are~~ were ~~non-~~karst areas. This study is the first time the model ~~is~~ has been used in a karst river basin~~ as an attempt in this study~~. ~~And the~~The structure of the model should be improved to suit the needs of the karst basin in questions. ~~So~~ Therefore, some effective measures should be taken before building the model. ~~Firstly~~First, ~~simplify~~ the karst water-bearing media should be simplified, and this process could include~~including~~ making the karst basin ~~as~~ a multiple and nested spatial structure~~,~~. The underground river could be included as the intelligible channel system in the model, and the cave could be used as the anisotropic medium with a large vertical infiltration coefficient and porosity but a small specific yield. Finally, the~~, and~~ fault could be used as the anisotropic medium with a ~~vertical,~~ large vertical infiltration coefficient and a specific yield. ~~Secondly~~Second, the ~~whole~~entire karst river basin ~~will~~ can be divided into many small karst sub-basins ~~by~~ using ~~the~~ high-resolution DEM data. Furthermore, ~~in order~~ to suit the karst area, the karst sub-basins ~~will~~ can be divided into many ~~karst hydrology respond units (~~KHRUs~~)~~, which are generally independent of each other. ~~And the whole~~The entire karst hydrological process, including the storage and regulation processes of the epikarst zone, the spatial interpolation of ~~the~~ precipitation, the evapotranspiration and the rainfall-runoff, are all calculated based on this KHRU. ~~After that~~Then, these hydrological processes ~~will~~ can be summarized ~~in~~ for each of the karst sub-basins. ~~Then~~Additionally, the outlet flow ~~will be~~is formed through the river confluence among each karst sub-basin from the upstream region to the downstream region. ~~Such~~ This type of~~a~~ multi-structure distributed hydrological model could utilize variously scaled information effectively and ~~make the best~~optimize the use of ~~the~~ observed meteorological, hydrological and geological data.

In this study, the KHRUs ~~are~~ were divided by GIS technology combined with karst topography, land use type and soil type (Ren, 2006). Each KHRU in this study ~~has~~ had its own model characteristics, such as ~~the~~ meteorological and hydrological characteristics, as well as the karst developmental characteristics~~ in this study~~. The KHRU ~~is~~ was proposed to describe the spatial variation of the karst sub-basins. ~~And make sure that the~~ The differences within the KHRUs ~~are~~ were smaller than ~~of~~those among the KHRUs. Then, ~~the~~ each KHRU ~~is~~ was vertically divided into ~~five~~5 layers~~ vertically~~: the canopy~~ layer~~, the soil~~ layer~~, the epikarst zone, the bedrock and the underground river. ~~The~~ A sketch map of the KHRU is as ~~follow~~follows:

a. The structure of the KHRU (Ren, Q.W.,2006) b. ~~The p~~Photograph of the three-dimensional ~~space~~ structure of the KHRU

Figure 10. Sketch map of the KHRU

~~Figure~~

In Figure ~~1~~10(~~.~~b), the three-dimensional~~ space~~ model of the KHRU in the ~~Liujiang Karst River Basin (~~LKRB~~)~~ ~~is~~ was built in the laboratory to better understand how groundwater ~~move~~moves in the karst media and ~~convert~~converges~~ mutually~~ with the surface river. Then, the hydrological model could be built ~~more~~ and visualized ~~through~~in this way.

~~In order to~~ To satisfy the applicability of the model in karst areas, the epikarst zone, which is~~ as~~ a distinctive structure of the KHRU, was carefully~~ is~~ considered ~~carefully~~ in the model. ~~It~~ The epikarst zone is composed of~~ the~~ karst rocks with macro cracks and tiny fissures. When ~~the~~ rain falls on the ground, it ~~will be~~is intercepted by plants, held in depressions ~~detention~~ and experiences some evapotranspiration~~ firstly~~. ~~After that~~Then, the rainfall ~~will~~ infiltrates into the soil and rock layer~~,~~ and ~~satisfy~~ satisfies the water shortage of the unsaturated zone. Part of the water in the epikarst zone may ~~formed the~~ form karst springs that emerge from the surface~~,~~. Another part will enter the ~~the~~ superficial karst water system of the epikarst zone. When the rainfall intensity is heavy enough to form ~~the~~ surface runoff on the exposed bedrock, part of the water will enter the karst conduit through ~~the~~ sinkholes.

The karst hydrological process of the epikarst zone could be divided into rapid fissure flow and slow fissure flow. After ~~the~~ heavy rain, a~~ lot~~ large amount of water in the epikarst zone is stagnant ~~in the epikarst zone~~ ~~could~~and can form a surface karst aquifer with a temporary water table. If there are large cracks or fractures under the water table, a precipitation funnel will ~~be formed~~form ~~along with~~and be associated with a drop in the water table~~ drops~~. ~~The r~~Rapid fissure flow ~~refer~~refers to ~~the~~ rainfall that infiltrates into the karst conduit through the precipitation funnel, ~~which~~ and this flow ~~happened~~occurs in the macro cracks and ~~had~~has ~~a fast~~high speeds. When ~~the~~ rainfall enters the superficial karst water system of the epikarst zone~~.~~, ~~T~~the macro cracks will ~~be~~ fill~~ed~~ ~~firstly~~first. This part of the saturated water content, named rapid fissure flow, will ~~go~~ move directly into the karst conduit through the macro crack. Because this rapid fissure flow will pass quickly through the karst conduit system without stopping, and because the water regulation and storage functions are ~~is~~ weak, ~~so ignored~~ the regulation and storage of the rapid fissure flow ~~was~~ were ignored in this study. The rest of the water content in the epikarst zone ~~keep infiltrating~~ infiltrates through ~~the~~ tiny fissures. This part of the water, named slow fissure flow, plays an important role in the process of rainfall regulation. The water content of the slow fissure flow ~~could~~can be described ~~as~~by the following equation:

$$SW_{epi} = Q_{\inf} - V_{crk}$$

(~~1~~4)

~~Where~~where SW_{epi} is the water content of the slow fissure flow in the epikarst zone.~~;~~

$Q_{\inf}$ is the infiltration water content of the rainfall, and V_{crk} is the water content of the rapid fissure flow in the macro crack.

The slow fissure flow in the epikarst zone is calculated by an exponential decay equation (Ren, 2006) as follows:

$$\begin{cases} W_{sep} = W_{epi}\left(1 - \exp\left(\dfrac{-\Delta T}{TT_{\text{perc}}}\right)\right) \\ W_{epi,\ t+1} = W_{epi,t} + SW_{epi,t+1} - W_{sep,t+1} \\ TT_{\text{perc}} = \dfrac{SAT_{epi}\text{-}FC_{epi}}{K_{epi}} \end{cases}$$

(~~2~~5)

~~Where~~where W_{sep} is the water content that flows from the epikarst zone to the underground river.~~;~~ ~~b~~Because the regulation and storage functions of the rapid fissure flow ~~is~~ are ignored in this study,~~ the~~ W_{sep} ~~means~~ refers to the slow fissure flow~~ here~~, W_{epi} is the current water content of the slow fissure flow, ΔT is the simulation time-step, TT_{perc} is the attenuation coefficient,

SAT_{epi} is the saturation water content of the slow fissure flow, FC_{epi} is the field capacity, and K_{epi} is the saturated hydraulic conductivity of the slow fissure flow.

The linear reservoir model is employed to calculate the regulation process of the superficial karst fissure system in the epikarst zone, and the base discharge is calculated by the hydraulic gradient of the KHRU (Neitsch et al.,2000) as follows~~:~~:

$$\begin{cases} Q_{gw} = 8000\dfrac{K_{epi}h_{wtbl}}{\left(L_{gw}\right)^2} \\ Q_{gw,i} = Q_{gw,i-1}\exp\left(-a_{gw}\Delta t\right) + W_{rchrg}\left[1-\exp\left(-a_{gw}\Delta t\right)\right] \\ W_{rchrg,i} = W_{seep}\left[1-\exp\left(-\dfrac{1}{\delta_{gw}}\right)\right] + W_{rchrg,i-1}\exp\left(-\dfrac{1}{\delta_{gw}}\right) \end{cases} \quad (~~3~~6)$$

~~Where~~where Q_{gw} is the base discharge, $Q_{gw,i}$ and $Q_{gw,i-1}$ ~~is~~ are the ~~supplies~~supply quantit~~y~~ies of the base discharge that ~~converge~~converges into the karst conduit or underground river on the i day and the (i-1) day, respectively, K_{epi} is the saturated hydraulic conductivity of the epikarst zone, h_{wtbl} is the hydraulic gradient, L_{gw} is the length of the KHRU, a_{gw} is the depletion coefficient of the base discharge, ΔT is the simulation time-step (day), $W_{rchrg,i}$ is the ~~supplies~~supply quantity of the aquifer on the i day (mm/d), W_{seep} is the water flux through the bottom of the soil profile into the underground aquifer on the i day ~~(~~(mm/d)~~)~~, and δ_{gw} is the delay time of the supply (day)~~supplies (day) day (day)~~.

In the original Liuxihe model, the underground layer is treated as an integral unit~~, a~~, and a linear reservoir method is used to calculate the underground runoff. However, the structure of the karst underground layer is non-linear; thus, the linear reservoir method is obviously not appropriate here. ~~So~~Therefore, in~~t~~ this study, the Muskingum routing method ~~is~~ was used to calculate the convergence process of the karst underground river~~ in this study~~, and the equation is as follows:

$$W = K[xI + (1-x)O] = KO' \quad (~~4~~7)$$

~~Where~~where O' is the water storage content, O is the outlet flow of the river reach, x is the dimensionless proportion factor, I is the inflow discharge of the river reach, and K is the slope of the correlation curve of the water storage content and the discharge.

The finite difference method is used to calculate the water balance equation and the Muskingum routing method:

$$\begin{cases} O_2 = C_0 I_2 + C_1 I_1 + C_2 O_1 \\ C_0 + C_1 + C_2 = 1 \end{cases}$$

~~(~~(~~5~~8) ~~)~~

~~where,~~ where

$$\begin{cases} C_0 = \dfrac{0.5\Delta t - Kx}{0.5\Delta t + K - Kx} \\ C_1 = \dfrac{0.5\Delta t + Kx}{0.5\Delta t + K - Kx} \\ C_2 = \dfrac{-0.5\Delta t + K - Kx}{0.5\Delta t + K - Kx} \end{cases}$$

~~(~~(~~6~~9)~~)~~

If the Muskingum routing method parameters of ~~the Muskingum routing method~~ *K* and *x* ~~could~~ can be determined for a karst underground river reach, then the values of ~~the~~ C_0, C_1 and C_2 ~~will~~ can be calculated by ~~the equatione~~Equation (6). When $\Delta t = 2Kx$, $C_0 = 0$, which means that the karst flood prediction lead time will be 2*Kx*. ~~; u~~Under this condition, ~~then~~ the Muskingum routing method can~~ould~~ be simplified as follows:

$$O_2 = C_1 I_1 + C_2 O_1$$

~~(~~(~~7~~10)~~)~~

One of the key problems of the Muskingum routing method ~~is to optimize~~involves determining how to optimize the parameters -*K* and *x* in ~~the~~ practical ~~application~~applications. ~~And i~~It is hard to ~~generalise~~generalize the parameters K and x in flood simulation and prediction due to their variability with flow conditions. Ahilan et al. (2012) used the generalized extreme value (GEV) to analy~~z~~se the flood frequency distributions in Irish rivers, and the result show~~ed~~s that a Type II distribution appears in a single cluster in the karst area, which reflects the finite nature of ~~K~~karst storage and the effects of saturation when storage is no longer available. In this study, 30 karst flood events are collected to validate the performance of the Muskingum model in study area. The least squares method is used to optimize the parameters -*K* and *x* in this study as follows:

~~The least square method is as used in this study:~~

$$\min\left\{E=\sum_{j=1}^{n}\{W_0(j)-W_1(j)-C]^{2}\right\}$$

~~(8)~~(11)

~~Where~~where E is the objective function between the observed water storage content and the simulated ~~one~~water storage content, which ~~makes~~requires only ~~require~~the least squares approximation with regard to the functional value~~,~~; $W_0(j)$ and $W_1(j)$ are the observed and simulated water storage contents ~~at~~ within the j period, respectively~~,~~; $W_1(j)=K[xI+(1-x)O]$;~~,~~ n is the total ~~numbers~~number of ~~the~~ observation periods~~,~~; and C is the absolute value of the water storage content.

~~In order to~~ To simplify ~~calculating~~the calculation, ~~making~~ $A=K*x$ and~~,~~ $B=K*(1\text{-}x)$;~~,~~ then, ~~taking~~ the partials can be taken with respect to A, B, and C, respectively:

$$\begin{cases}\sum W_0 I = A\sum I^2 + B\sum(OI) + C\sum I^2 \\ \sum W_0 O = A\sum(OI) + B\sum O^2 + C\sum O \\ \sum W_0 I = A\sum I + B\sum O + Cn\end{cases} \qquad \text{~~(9)~~(12)}$$

Then, the values of A, B, and C ~~could~~ can be calculated as follows:

$$\begin{cases}A=\dfrac{y_1}{y_2}-\dfrac{y_3}{y_2} \\ B=\dfrac{y_1 z_2}{y_3 z_2}-\dfrac{y_2 z_1}{y_2 z_3} \\ C=\sum\dfrac{W_0 - A\sum I - B\sum O}{n}\end{cases}$$

~~(10)~~(13)

~~Where~~where~~,~~

$$
\begin{cases}
y_1 = \sum (W_0 I) - \dfrac{\sum W_0 \sum I}{n} \\
y_2 = \sum I^2 - \dfrac{(\sum I)^2}{n} \\
y_3 = \sum (IO) - \dfrac{\sum O \sum I}{n} \\
z_1 = \sum (W_0 O) - \dfrac{\sum W_0 \sum O}{n} \\
z_2 = \sum O^2 - \dfrac{(\sum O)^2}{n} \\
z_3 = \sum IO - (\dfrac{\sum O \sum I}{n}) \\
K = A + B \\
x = \dfrac{K}{A}
\end{cases}
$$

~~(~~(~~11~~14)~~)~~

The parameters of the Muskingum routing method ~~could~~ can be optimized ~~through~~ using the ~~above~~ equations shown above. ~~And after~~ ~~After that~~Then, the convergence process of the karst underground river ~~could~~ can be calculated by the Muskingum routing method in the Liuxihe model.

5 Model set up

5.1 ~~h~~Hydrological model setup

The method ~~combining~~that combines a DEM with a stream network leads to a more accurate drainage network ~~from~~ in terms of surface runoff modelling (Li and Tao,2000), especially in karst ~~area~~areas. In this study, ~~according to~~based on the high resolution of ~~200m*200m~~200 m×200 m used for the Liuxihe model in the LKRB, the ~~whole~~entire studied area ~~is~~ was divided into 1,469,900 grid cells, which were named the karst sub-basins, ~~by~~ using the DEM. The grid cells included 1,463,204 hill slope cells and 6,696 river cells. Then, the karst sub-basins ~~will be~~were further divided into many ~~karst hydrology respondresponse units (~~KHRUs~~)~~ ~~further~~; ~~, with~~ ~~the~~ an example KHRU is ~~is as~~ shown in Figure 1. The river system ~~is~~ was ~~divide~~divided into three~~-~~ orders as shown in Figure 3.

In the Liuxihe model, the flood process of ~~some special~~specific points, named the early warning points ~~on~~ of the river section, could be simulated and predicted. ~~From~~ Figure 3~~, it can be seen~~ shows that there are few rain gauges located ~~along the~~ upstream of the Liujiang ~~river (that~~River (which is why the PERSIANN-CCS QPEs ~~is~~were used here). However, the karst is very developed here, and the influence of the karst ~~dominate~~dominates the runoff processes ~~a lot. So a~~. Therefore, an early warning point ~~is set up~~was established at the Danian ~~river~~ River gauge (Figure 3)~~.~~, and a sub-karst basin of the upstream area could be divided from this early warning point. ~~And 10~~ Ten karst flood events ~~will be~~were collected to validate the performance of the model~~ performance~~.

Because of the sinkholes and karst depressions in the karst watershed, as well as the systematic error of the DEM itself, there are many pits, including ~~the~~ true and false pits, in the LKRB. Among them, the true pits ~~are~~ include ~~the~~ karst depressions and sinkholes~~,~~, and they usually have a certain scale ~~with~~ and elevational ~~difference. While the~~ differences. The false pits ~~are~~were ~~only~~ represented only by ~~just only~~ a few points with low elevation, which ~~is~~ was due to the systematic errors of the DEM. ~~So~~Therefore, the true and false pits should be reliably distinguished ~~reliably~~ before using the DEM data to divide the area into the karst sub-basins. ~~Firstly, finding out all~~ First, we identified all of the pits with low elevation~~,~~ and ~~connect~~connected them ~~into~~ on a plane.~~;~~ ~~t~~Then, we ~~distinguish~~distinguished the true pits from the false ~~ones~~pits ~~according to~~based on the on-site topographic survey. Finally, ~~keeping~~ the model retained the true pits ~~like~~ such as the sinkholes and karst depressions, ~~unchanged~~ but ~~filling~~ the false pits ~~in the model~~were filled (i.e., removed).

The ~~karst hydrology respond unit (~~KHRU~~)~~ ~~is~~ was introduced in this study to reasonably describe the spatial variability of the karst water-bearing media (as shown in ~~Figure1~~Figure 1). The spatial ~~characteristic~~characteristics of every KHRU ~~has~~have a definite physical meaning. ~~So~~Therefore, the calculation of the evapotranspiration, rainfall-runoff and parameter optimization ~~on~~ of the KHRU ~~is also~~was physically based, which could truly reflect the differences of the underlying surface. After the division of the karst sub-basins and the KHRUs, the post-processed PERSIANN-CCS ~~QPEs~~QPE results ~~will~~ can be used as the input data for the Liuxihe model to simulate and forecast the karst flood process. The performance of the ~~coupling~~ coupled model ~~could be~~was reliably improved ~~reliably~~ in this way.

The early warning points set in the Liuxihe model could offer ~~an~~ important alerting and forecasting information ~~on~~ for some critical river sections. In this study, a key early warning point named Goutan (Figure 1a, b) is set to extract the most developed karst area in the LKRB- Beijiang catchment, where the influence of karst features highly dominates the rainfall-runoff ~~-runoff~~ processes. There are 11 early warning points ~~are~~ set in the Beijiang catchment (Figure 1b).

5.2 Parameter optimization of the ~~coupling~~ coupled model

There ~~are~~ were 14 parameters that needed to be optimized for the original Liuxihe model, and after adding the karst mechanism, the number of ~~the~~ parameters ~~is~~ increased to 20, as shown in Table 2. The parameters of the epikarst zone ~~are~~ were the most complicated due to the anisotropy of the karst water-bearing media, which ~~makes~~ made it ~~hard~~difficult to measure and calculate the hydraulic characteristics.

The hydrogeology parameters used in this study, including the permeability coefficient of the rock mass, the rainfall infiltration coefficient, the specific yield of the aquifer, and the storage coefficient, ~~are~~ were calculated by the field test and the experience function. For instance, the permeability coefficient ~~/~~K ~~is~~ was calculated by an experience function according to the water inrush prediction of a coal mine in the study area~~.~~:

$$\begin{cases} Q = 1.366K\dfrac{(2H-M)*M-h^2}{\lg R_0 - \lg r_0} * \dfrac{1}{24} \\ R_0 = r_0 + 10*S\sqrt{K} \\ r_0 = \sqrt{\dfrac{a*b}{\pi}} \end{cases} \quad (~~12~~15)$$

~~Where,~~where Q is the mine inflow, m^3/h~~,~~; K is the permeability coefficient, m/d~~,~~; H is the distance from ~~the~~ the water-resisting floor to the water level of the confined aquifer, m~~,~~; M is the aquifer thickness~~,~~, m~~,~~; h is the height of the dynamic water level, m~~,~~; R_0 ~~—~~ is the substitute influence radius, m~~,~~; r_0 is the substitute radius, m~~, —~~ S is the drawdown value, m~~,~~; and $a*b$ is the area of the mine, m^2.

~~–~~In the water inrush test of the coal mine, the ~~others~~other parameters in ~~equation~~ Equation (~~12~~15) ~~are~~ were given, and the permeability coefficient ~~/~~K ~~couldcan~~was ~~be~~ calculated by ~~the~~ anti-~~equation~~ Equation (~~12~~15).

The parameters of the epikarst zone, including the thickness~~, Saturated~~, saturated water content~~,~~ ~~, Field~~field capacity and macro crack volume ratio~~, and so on~~ ~~are~~ were obtained ~~according to~~based on the field survey, geological borehole test and pumping test~~,~~ as well as on the empirical value observed in the study area.

The epikarst zone ~~is~~ was mainly developed on the hard surface of pure carbonate rock, especially on ~~the~~ Paleozoic limestone. The thicknesses and characteristics of the epikarst zone ~~are different~~differ due to ~~the~~ different climates, topography and landforms.~~—~~ The parameters of the ~~coupling~~ coupled model and the epikarst zone are listed ~~inTable~~ in Table 2(a) and (b)~~-~~, and the rainfall infiltration coefficients of the different karst landforms ~~is~~ are calculated based on the empirical values shown in Table 2(c).

(a) The parameters of the coupling model

(b) The physical parameters of the epikarst zone

(c)The rainfall infiltration coefficient of different karst landforms

Table ~~–~~2~~-~~. The parameters of the model

The soil type parameters~~, of the Soil type like~~ such as the saturated water content and the field capacity, ~~are~~ were calculated ~~through~~using a software tool (Ren, 2006). ~~.~~The statistical relationship between the soil texture and the soil water ~~could~~can be easily queried ~~easily~~ in the software tool.~~And~~ In addition, ~~it~~ this method has been effectively ~~proved~~proven by many experiments (Servat and Sakho, 1995), and the calculated value of this method has a good fitting relationship with the measured value.

The Liuxihe ~~Model~~ model has been deployed on a supercomputer system with parallel computation technology (Chen et al., 2011). An improved PSO algorithm (Chen et al., 2017) ~~is~~ was employed to optimize the parameters of the ~~coupling~~ coupled model in this study. There are 30 karst flood events from 1982-2013 in the LKRB, and among them, 3 flood events—Floods 2004070300, 2009060908, and 2011010100—~~are~~were used for parameter optimization ~~including the Flood 2004070300,2009060908, and 2011010100 are~~ simulations~~ed~~ in this paper. The flood simulation results are shown in Figure 11 and Table 3.

Figure 11. The flood simulation results obtained through parameter optimization by the improved PSO algorithm

From the flood simulation results in Figure 11, it can be seen that the Flood 2009060908 simulated result is the best. The simulated ~~flood~~ process for this flood is closest to the observed~~r one~~ process, and the valuation indices of flood simulation results including the Nash–Sutcliffe~~-Suteliffe~~ coefficient, C; correlation coefficient, R; process relative error, P%; peak flow relative error, E%; ~~The~~ coefficient of water balance, W; and peak time error, T(h), are also the best. Table 3 shows the valuation indices of flood simulation results ~~by~~ from the improved PSO algorithm. Therefore, ~~this~~ Flood 2009060908 is finally adopted for the Liuxihe model parameter optimization. Other floods will be used to verify the model performance.

Table 3. The evaluation indices of flood simulation results obtained through parameter optimization by the improved PSO algorithm

The parameter optimization results ~~by~~ from the improved PSO algorithm are shown in Figure 12 as follows~~., And the The flood process for parameter optimization is was the Flood 2009060908. The results of parametersparameter optimization are shown in Figure 10, among them,~~ : (a) ~~is~~ the objective function evolution result, (b) ~~is~~ the ~~parameters~~parameter evolution result, and (c) ~~is~~ the simulated flood process ~~by~~ using the optimized model parameters.

Figure 12. Parameter optimization results with the improved PSO algorithm

~~In order to~~

To test the parameter~~s~~ optimization effect with different precipitation sources, both the precipitation of the rain gauge and the precipitation of the PERSIANN-CCS QPEs ~~are~~ were used to optimize the parameters of the ~~coupling~~ coupled model. ~~To compare with that~~For comparison, the simulated flood process of the coupled~~ing~~ model with the same parameter ~~as that~~ from the rain gauges and the re-optimized parameter ~~with~~ from ~~the the~~ the post-processed PERSIANN-~~-~~CCS QPEs are ~~also~~ drawn in Figure 10(c).~~–~~

5.3 Parametric uncertainty analysis

In this study, ~~The~~ parametric uncertainty analysis ~~in this study is refer~~ refers to ~~the~~ sensitivity analysis, ~~which~~ and this process is conducted using a fixed module called the parametric sensitivity analysis sub-model in the Liuxihe model~~,~~. ~~it~~It is a parameter sensitivity analysis method that was developed based on the GLUE method, and it was named ~~Multi~~multi-~~Parameter~~ parameter ~~Sensitivity~~ sensitivity ~~Analysis~~ analysis (MPSA) by Choi (1999) et al. Monte Carlo sampling ~~is~~ was used to obtain the value of the parameter spatial variation~~value~~. ~~And the~~The sensitivity of each parameter could be obtained ~~through~~ by running the model multiple times~~runs of the model~~.

In this study, the Nash–Sutcliffe coefficient ~~is~~ was used as the objective function value for the parametric sensitivity analysis, and the formula is as follows:

$$NSE = 1 - \frac{\sum_{i=1}^{n}\left(Q_i - Q_i^{'}\right)^2}{\sum_{i=1}^{n}\left(Q_i - \overline{Q}\right)^2}$$

(~~13~~16)

~~Where,~~where NSE is the objective function value of the Nash–Sutcliffe coefficient, Q_i and $Q_i^{'}$ are the observed streamflow and the simulated ~~one~~streamflow, respectively, in m^3/s, $\overline{Q}$ is the average value of the observed flows in~~,~~ m^3/s, and n is the number of observation periods in~~,~~ hours.

~~Firstly~~First, the~~determine the~~ initial ~~values~~value range of the parameter ~~is~~was determined to be [0.5,2.5]. ~~Secondly~~Second, 6,000 groups of parameter sequences were obtained by the Monte Carlo sampling method. ~~Thirdly~~Third, ~~run~~ the Liuxihe model was run to simulate the objective function values of the Nash–Sutcliffe coefficient, and the karst flood processes ~~are~~ were ~~also~~ the three flood events also used for parameter optimization. In this study, ~~T~~the critical value of the Nash–Sutcliffe coefficient ~~is~~ was 0.85~~ in this study~~, and the objective function values~~ that~~ below this threshold ~~are~~ were considered ~~as the~~to be unacceptable values~~,~~; otherwise, they ~~are the~~were considered to be acceptable values. The degree of separation between ~~them~~ these values indicates the sensitivity of the parameters. ~~And this~~ This degree of separation ~~degree is~~ was calculated according to the Nash–~~-~~Sutcliffe coefficient (NSD)~~, NSD, for short~~. ~~In order to~~ To ~~analyze~~analyse ~~the~~ parameter sensitivity ~~easier~~more easily, a factor SI is given here, and SI=1- |NSD|~~;~~, ~~—~~the closer ~~is this~~ the value of SI is ~~is~~ to 0, the less sensitive ~~is~~ the~~is~~ parameter~~ is~~. Table ~~3~~ 4 shows the SI values~~ of SI~~, which represent the sensitivity of the parameters in the Liuxihe model.

Table 4. The ~~sensitivity~~ calculation results of the parameters sensitivity in the Liuxihe model

6 Results and discussion~~s~~

6.1 Results of ~~parameters~~parameter optimization and sensitivity analysis ~~results~~

The results of ~~parameters~~the parameter optimization are shown in Figure ~~10~~12 as follows~~, among them,~~: (a) ~~is~~ the objective function evolution result and~~,~~ (b) ~~is~~ the ~~parameters~~parameter evolution result~~,~~. ~~And from~~ From the results of Figure ~~10~~12(a) and (b), it ~~could~~can be ~~found~~ seen that the evolution number of the objective function for the parameter was~~s is~~ 50~~ times~~, and the computation time of the ~~parameters~~parameter optimization based on the improved PSO algorithm ~~is~~ was ~~about~~approximately 8 hours, which means that ~~the~~ convergence of the ~~parameters~~parameter optimization was achieved ~~just~~ after only 50 cycles. ~~And compared~~ In comparison,~~with that,~~ the computation time of the initial model parameters that ~~are~~ were not optimized ~~is~~ was ~~about~~approximately 55 hours. ~~It~~This result implies that the improved PSO algorithm ~~has~~ had high efficiency in terms of ~~parameters~~parameter optimization.

~~In order to~~To test the parameter~~s~~ optimization effect ~~with~~ using the improved PSO algorithm (Chen et al., 2017), the flood process simulated results ~~by~~ achieved from~~using~~ the improved PSO algorithm, as well as the initial model parameter values, are shown in Figure ~~10~~12(c)~~ ~~. ~~And from~~ From the results ~~of~~ shown in Figure ~~10~~12(c), it ~~could~~can be ~~found~~ seen that the ~~coupling~~ coupled model does not simulate the observed karst flood process well when the~~with~~ initial model parameter values are ~~does not simulate the observed karst flood process satisfactorily~~~~were used~~~~;~~. ~~a~~Additionally, ~~and compared with that,~~ the simulated flood process ~~by~~ obtained from using the improved PSO algorithm ~~is~~ was very close to that from the observed process, which means that the improved PSO algorithm (Chen et al., 2017) in this study ~~is~~ was effective~~,~~ and could largely improve the performance of the coupled model~~coupling model's performance~~.

In this study, the sensitivity of the parameters in the Liuxihe model ~~is~~ was calculated according to the Nash~~ ~~–Sutcliffe coefficient, as shown in Equation~~formula~~ (~~13~~16). The values of SI =1- |NSD|, which represent the sensitivity of the parameters, and ~~according to~~ the results in Table ~~3~~ 4 indicate that~~,~~ the SI values of the ~~parameter Saturated~~ saturated water content~~/θsat~~ parameter, θsat, were maximized~~are the maximum~~, which means that the degree of separation ~~degree of the~~between the unacceptable values and the acceptable ~~ones~~ values (NSD) ~~are the~~was minimal~~minimum.~~. ~~It means that this~~This parameter~~/~~, θsat, ~~is~~ was the most sensitive parameter in the Liuxihe model. When the SI value of ~~the SI for~~ a parameter is greater than 0.7, this parameter ~~in the Liuxihe model~~ is identified as a highly sensitive parameter in the Liuxihe model, and ~~the~~ SI values ~~of the SI~~ between 0.2 and 0.7 indicate that a~~, this~~ parameter ~~is~~ has medium ~~sensitive~~sensitivity. When the SI value ~~of the SI~~ is less than 0.2, the parameter is insensitive. From Table 3, the SI values of ~~the SI for~~the different parameters, from ~~big~~ largest to smallest, are the ~~Saturated~~ saturated water content~~/~~, θsat > ~~Saturation~~ saturation permeability coefficient~~/~~, θs > ~~Field~~ field capacity~~/~~, θfc > ~~Saturated~~ saturated hydraulic conductivity~~/~~, Ks > ~~Macro~~ macro crack volume ratio~~/~~, V > Muskingum routing method (t~~T~~he slope of the water storage content and flow curve)~~/~~, K > Muskingum routing method (the proportion of the flow), ~~/~~χ > ~~Soil~~ soil layer thickness~~/~~, z > ~~Soil~~ soil coefficient, ~~/~~b > ~~Bottom~~ bottom width, ~~/~~Sw > ~~Bottom~~ bottom slope, ~~/~~Sp > ~~Slope~~ slope roughness, ~~/~~n > ~~Channel~~ channel roughness, ~~/~~n_1 > ~~Depletion~~ depletion coefficient, ~~/~~ω > ~~Evaporation~~ evaporation coefficient, ~~/~~λ > ~~Potential~~ potential evaporation, ~~/~~Ep > ~~Wilting~~ wilting percentage, ~~/~~Cwl~~, among them,~~. Additionally, the ~~parameters –~~θsat, θs, θfc, Ks~~,~~, V, K, and χ parameters were~~are~~ highly sensitive; the z, b, Sw, Sp, n~~,~~, n1 and ω parameters had medium sensitivity~~are medium sensitive,~~; and the λ, Ep~~,~~, and Cwl ~~are~~ parameters were insensitive ~~parameters~~.

The ~~parameters – F~~flow direction, ~~Slope~~ slope and ~~the T~~thickness parameters of the epikarst zone ~~are unadjustable~~could not be adjusted~~,~~. ~~a~~Among them, the ~~Flow~~ flow direction and the ~~S~~slope ~~are~~ were directly calculated by the DEM data ~~directly~~, and the ~~Thickness~~ thickness of the epikarst zone ~~is~~ was a fixed value ~~in~~ for a particular region. It ~~is~~ was ~~about~~approximately 3-10 ~~meter~~ metres ~~in~~ of the study area according to the field survey.

6.2 Model validation results

To better test the effect of the Liuxihe model in flood simulation and prediction~~,~~ and to increase ~~make~~ the results ~~more acceptibility~~acceptability~~ed~~, ~~there are~~ 30 karst flood events from 1982-2013 in LKRB are simulated by the Liuxihe model, and the evaluation indices of the simulated flood results are listed in Table 5. ~~And fFrom~~ Table 5, ~~it can be seen~~ shows that the 6 evaluation indices of the flood simulation results for the 30 flood events are credible and reasonable. The average value of the Nash–Sutcliffe coefficient (C) is 0.82, the correlation coefficient (R) is 0.83, the process relative error (P) is 0.22, the peak flow relative error (E) is 0.05, the water balance coefficient (W) is 0.87, and the peak flow time error (T) is -6 hours~~, respectively,~~. ~~a~~Among these results~~m~~, the peak flow relative error (E) is minimal. The applicability of the Liuxihe model is prove~~d~~n through these accepted flood simulation effects in the LKRB.

Table 5. The evaluation indices of the simulated flood results based on the Liuxihe model in the LKRB

~~In order t~~To further validate the performance of the Liuxihe model in flood simulation and prediction, simulations are performed in a very developed karst area, where the influence of karst landforms plays an important role in hydrological processes. ~~In this study, t~~The most developed karst area in the whole basin examined in this study is the Beijiang catchment, and it is divided by the early warning point- Goutan set in the Liuxihe model (Figure 1b). ~~And~~ In total, 10 karst flood events are simulated to test the performance of the Liuxihe model, and the evaluation indices of the simulated flood results are shown in Table 6~~,~~. ~~among~~ From these results~~m~~, 4 karst flood simulation results are shown in Figure 13.

Table 6. The evaluation indices of the simulated flood results based on the Liuxihe model in the Beijiang catchment

Figure 13. Four~~4~~ karst flood simulation results produced by the Liuxihe model in the Beijiang catchment

From the results in Table 4, the evaluation indices of the simulated karst flood results produced by the Liuxihe model are quite good in the Beijiang catchment. The average value of the Nash–Sutcliffe coefficient (C) is 0.92, the correlation coefficient (R) is 0.91, the process relative error (P) is 0.11, the peak flow relative error (E) is 0.08, the water balance coefficient (W) is 0.94, and the peak flow time error (T) is 3 hours~~, respectively~~. It is obvious that the evaluation indices of the simulated karst flood events based on the Liuxihe model are satisfying, and the accuracy is very high.

~~Also,~~Additionally, from the flood simulation results in Figure 13, the 4 reasonable karst flood simulation results including those for floods 2008071311, 2012080310, 2014061015, and 2016091501 prove~~d that~~ the performance of the Liuxihe model in karst areas. The simulated flood discharge processes are very close to the observed values, especially for the peak flows. ~~So it~~ This finding implies that the Liuxihe model is feasible and effective in flood simulation and prediction in areas where karst is very well developed, as in the ~~just like~~ Beijiang catchment.

6.~~2~~3 Results of flood simulation with the post-processed PERSIANN-CCS QPEs

After the correction was made, the post-processed PERSIANN-CCS ~~QPEs~~QPE precipitation ~~has become~~ became much closer to the ~~observed~~ precipitation observed ~~of~~at the rain gauge. ~~In order to~~ To ~~analyze~~analyse the effects of flood simulation with the initial PERSIANN-CCS QPEs and the post-processed QPEs, ~~five~~5 karst flood events, including ~~F~~Floods 200806090200, 200906090800, 201106010900, 201206022000 and 201306011400, ~~are~~ were simulated and ~~are~~ compared; the results are shown –in Figure ~~11~~14. In this simulation, ~~maintaining~~ the ~~coupling~~ coupled model parameters remained unchanged;~~,~~ i.e., ~~means~~ the original ~~coupling~~ coupled model parameters ~~with~~ based on the rain ~~gauges~~gauge precipitation were employed, ~~not~~ while the re-optimized model parameters ~~with~~ based on the precipitation of the post-processed PERSIANN-CCS QPEs were not.

Figure 14. The flood simulation results of the coupl~~ing~~ed model ~~with~~ using two precipitation products

~~From the result of~~ Figure ~~11~~ 14 shows~~, it could be seen~~ that the karst flood simulation results ~~with~~ from the initial PERSIANN-CCS QPEs ~~are~~ were not ~~so~~ satisfactory, and the performance of the model ~~are~~was worse than that of the rain gauge precipitation. For instance, the simulated peak flows ~~with~~ from the PERSIANN-CCS QPEs ~~are~~ were lower than the observed ~~ones~~peak flows. ~~While t~~The performance of the coupled~~ing~~ model with the post-processed PERSIANN-CCS QPEs ~~is~~ was much better, and ~~also~~ the evaluation indices of the flood simulation ~~have been~~were largely improved (as shown in Table ~~3~~7). The average value of the Nash–Sutcliffe coefficient (C) ~~has a~~increased by 7%~~ increase~~, the correlation coefficient (R) increased by~~has a~~ 8%~~ increase~~, the process relative error (P) ~~has a~~decreased by 6%~~ decrease~~, the peak flow relative error (E) ~~has a~~decreased by 14%~~ decrease~~, the water balance coefficient (W) ~~has a~~increased by 5%~~ increase~~, and~~—~~ the peak flow time error (T) ~~has~~ had a decrease of ~~7~~2 ~~-~~hours~~ decrease, respectively~~. Among ~~them~~these parameters, the peak flow relative error ~~has~~ had the ~~biggest~~largest improvement, ~~which is~~making it the most ~~concerned~~important factor in flood prediction. It ~~is~~ was obvious that the evaluation indices ~~are~~ improved substantially ~~with~~ when the~~the~~ post-processed QPEs were used. ~~So it implies~~ Therefore, the post-process~~ed~~ing method for PERSIANN-CCS QPEs in this paper ~~is~~ was feasible and effective. ~~And~~In addition, coupling the post-processed PERSIANN-CCS QPEs with the Liuxihe model has the potential to improve the model performance in ~~in for~~ flood simulation and prediction in the LKRB.

Table 7. Evaluation indices of simulated flood events with the initial PERSIANN-CCS QPEs and the post-processed values~~ones~~

~~Table .~~

~~:~~

6.~~3~~4 ~~Effects e~~Comparisons of different model parameters

~~——~~The model parameters that were optimized ~~with~~ using the precipitation ~~of~~ from the rain gauge and those optimized using the PERSIANN-CCS QPEs ~~are~~ were different, and the performance of the ~~coupling~~ coupled model ~~with~~ using the different parameters ~~makes~~ made a ~~big~~large difference in the flood simulation and prediction. To analyse this effect, the flood simulation results ~~with~~ from two different sets of model parameters are shown in Figure ~~12~~15. One set ~~is~~ used the parameters of the ~~coupling~~ coupled model that was optimized by the precipitation ~~of~~ from the rain gauge;~~,~~ i.e., ~~means~~ the coupled flood simulation results ~~with~~ had used the same parameter as the rain gauge precipitation. ~~And the~~The other ~~is~~ used the parameters that were re-optimized by the post-processed PERSIANN-CCS QPEs. The flood process used for ~~re-~~parameter reoptimization~~-optimization~~ ~~is~~ was also ~~the~~ Flood 2009060908, and the other four flood events ~~are~~ were used to validate the performance of the ~~coupling~~ coupled model.

Figure ~~–~~15. Coupled flood simulation results ~~with~~ using the same parameter as the rain gauge precipitation and the re-optimized parameter ~~with~~ from the post-processed PERSIANN-CCS QPEs

~~From the above results in Figure 12, it has been found~~Figure ~~12~~15 shows that the simulated flood results ~~with~~ obtained using the re-optimized parameters ~~by~~ from the post-processed

PERSIANN-CCS QPEs ~~are~~ were much better than ~~that of~~ those ~~with~~ obtained using the same parameter as the rain gauge precipitation. The simulated flood discharge processes, especially the peak flows with the re-optimized parameter, ~~are~~ were closer to the ~~observation~~ observed values. To further compare the flood simulation results, six evaluation indices ~~are~~ were calculated and are shown in Table ~~4~~8~~, the~~. The average value of the Nash–Sutcliffe coefficient ~~has a~~increased by 7% ~~increase~~, the correlation coefficient ~~has a~~increased by ~~6~~7%~~ increase~~, the process relative error ~~has a~~decreased by 2%~~ decrease~~, the peak flow relative error ~~has a~~decreased by 4%~~ decrease~~, the water balance coefficient ~~has a~~increased by ~~2~~3%~~ increase~~, and the peak flow time error ~~has~~ ~~had~~exhibited a ~~18~~3 ~~hours~~-hour decrease~~, respectively.~~ .

Table 8. The effect of recalibrating the coupling model parameters

~~What is more, comparing~~

Moreover, compared with the simulated flood results ~~of~~ from the initial PERSIANN-CCS QPEs in Table ~~3~~8, the flood simulation results with the re-optimized parameters ~~by~~ from the post-processed PERSIANN-CCS QPEs made ~~a~~ great progress~~:~~. ~~t~~The average value of the Nash–Sutcliffe coefficient ~~has a~~increased by 14%~~ increase~~, the correlation coefficient ~~has a~~increased by ~~14~~15% ~~increase~~, the process relative error ~~has~~ decreased by~~a~~ 8%~~ decrease~~, the peak flow relative error decreased by~~has a~~ 18%~~ decrease~~, the water balance coefficient ~~has a~~increased by ~~7~~8%~~ increase~~, and the peak flow time error ~~has~~ had a ~~25~~5 ~~hours~~ -hour decrease~~, respectively~~ (as shown in Table ~~3~~ 7 and Table ~~4~~8). ~~So it implies~~These results imply that the re-optimized parameters ~~with~~ calculated using the post-processed PERSIANN-CCS QPEs are necessary and effective for the ~~coupling~~ coupled model~~ are necessary and effective~~, ~~which makes a~~and the model performance improved ~~better performance for the coupling model~~ in terms of karst flood simulation and prediction.

6.~~3~~ 5 Peak flow time error analysis

It is very important to accurately determine the flood peak flow time in karst ~~area~~areas, ~~which~~ as this information could ~~offer enough~~improve the response times ~~for~~ of safe and rapid evacuations ~~evacuation safely and rapidly~~ before ~~the~~ a flood disaster appears. ~~From the above results in~~As shown in Figures ~~11~~ 14 and~~,~~ ~~12~~ 15 and in Tables ~~3~~7~~,~~ and ~~4~~8, ~~it has been found that~~ all flood simulations ~~have~~ had significant peak flow time errors, and all of ~~them~~ the errors were~~are~~ negative, ~~means~~indicating that the simulated flood peaks appeared earlier than did the peaks in the observed values. Among them, the average peak flow time error ~~with~~ from the precipitation ~~of~~ from the rain gauge ~~is~~ was -7 hours, ~~and that~~ and this value ~~is~~ was -~~32~~ 10 hours ~~with~~ when the precipitation ~~of~~ from the initial PERSIANN-CCS QPEs was used. ~~It~~ This is an obvious error and ~~could not~~ cannot be ignored in flood prediction. ~~While the~~ The average peak flow time error of the ~~coupling~~ coupled model ~~with~~ that used the post-processed PERSIANN-CCS ~~QPEs~~QPE precipitation and re-optimized parameters ~~is~~ was ~~also~~ -~~7~~ 5 hours. ~~It~~This result indicates that there is~~makes~~ a great difference. It has been found that ~~both~~ the average peak flow time errors of the Liuxihe model ~~with~~ generated from the precipitation ~~of~~ from the rain gauge and from the ~~coupling~~ coupled model ~~with~~ that used the precipitation ~~of~~ from the post-processed PERSIANN-CCS QPEs and re-optimized parameters ~~are~~ were -5 to -7 hours (as shown in Table ~~4~~7 and 8). ~~So it implies~~ Therefore, the peak flow time error ~~is~~ was -5 to -7 hours for the ~~coupling~~ coupled model in the LKRB, which means that the actual time of the flood peak may be 5-7 hours later~~,~~ ~~.~~; ~~t~~This value is~~which is~~ very important in flood prediction and is equivalent to a 5-7~~ hours long ~~-hour lead time in which safe evacuations can occur~~for evacuation safely~~.

There are two reasons for the peak flow time errors. One reason is the systematic error of the ~~coupling~~ coupled model itself.~~ And that~~ This error could be reduced by improving the model structure and function as well as by the reliable precipitation~~ by~~ from the PERSIANN-CCS QPEs and ~~parameters~~parameter optimization. The other reason is due to the karst development laws and the characteristics of karst water-bearing media, which can regulate the rainfall process during floods. The karst depressions and other ~~karst~~ negative landforms in the upstream regions can hold back and store ~~some~~ large amounts of ~~floods~~floodwater. ~~What is more, the~~ Furthermore, karst fissures can also slow ~~down~~ the ~~floods~~flood rate. These factors can play a crucial role in detaining natural floods and clipping the flood peaks~~ detention and peak clipping~~. ~~So~~Therefore, the response times of the flood peak flow to the rainfall increased, and the observed flood peak times lagged behind. In comparison, the simulated flood peak flows appeared earlier~~ ahead of time~~.

~~The rainfall process~~As rainfall moves from the sky to the ground and, finally, to the point where the rainfall converges ~~to~~ at the outlet of the basin, it has passed through the surface karst zone, the karst conduit and fissure~~,~~ as well as the underground river. ~~And the~~ The karst development laws and the characteristics of the karst water-bearing media have an obvious influence on the rainfall-runoff~~-runoff~~ process during the ~~whole~~entire hydrological process, which ~~makes~~increases the response time of the flood peak flow to rainfall~~ increases~~, and the simulated flood peak flow ~~by~~ in the ~~coupling~~ coupled model appears earlier. ~~It~~This result implies that there is a lead time ~~for~~ that can be used for safe evacuation measures~~evacuation safely in flood prediction~~.

The flood peak flow time has a very close relationship with the ~~floods~~flood rate, and the ~~floods~~flood rate is very important ~~to determine~~in determining the key factors of the karst conduit, the underground river and the other hydrogeological parameters. The sensitive parameters in this paper, such as the underground river parameters (as shown in Table 2), could be ~~estimate~~estimated from the ~~floods~~flood rate to build the ~~coupling~~ coupled model in the karst area~~s~~. According to the survey data and the tracing test in the study area, i.e., the LKRB, the flood flow rate ~~of floods~~ is ~~about~~approximately 8.64-17.~~28km/d~~28 km/d in the dry season~~; that,~~ ~~is~~ 17.28-43.2 km/d in the normal season and ~~is~~ 43.2-129.6 km/d in the flood period. The extreme flow rate can reach 172.~~8km/d, means~~8 km/d, indicating that the karst conduit is ~~very~~ highly developed in the LKRB.

7 Conclusion

~~There is no very~~ L~~l~~ittle reliable precipitation data ~~of~~ from rain gauges are available in ~~many~~ most karst river basins. How to obtain ~~the~~ reasonable rainfall data for the development of a hydrological model that can be used for~~in~~ flood prediction is especially important. In this study, the PERSIANN-CCS QPEs ~~could~~ offered effective precipitation results for the study area. ~~And after~~ After the correction, the post-processed PERSIANN-CCS QPEs coupled with a distributed hydrological model~~-~~, i.e., the Liuxihe model, ~~is~~were proposed ~~in~~ for karst flood simulation and prediction in the LKRB. The purpose ~~is~~ of the study was not only to simulate the flood process well~~,~~ but also to ~~find out~~determine ~~the key factor~~key information about how the karst hydrological process responds to the rainfall process in the ~~coupling~~ coupled model. The ~~coupling~~ coupled model employed in this paper h~~as~~ad ~~a~~ good performance in ~~in~~ simulating flood ~~events simulation~~events; thus, this method offers~~which can offer~~ ~~a~~ reasonable theoretical guidance for flood prediction, control and disaster reduction in karst river basins ~~like~~ such as the LKRB. Based on the study results, the following conclusions ~~could~~can be drawn:

1). The quantitative precipitation estimates produced by the PERSIANN-CCS QPEs ~~are~~ were ~~quite~~ very similar to the observed precipitation ~~by~~ from the rain gauges, especially in terms of~~the~~ rainfall distribution. ~~But~~However, the PERSIANN-CCS QPEs ~~underestimates~~underestimated the precipitation value. The average precipitation ~~is~~ was ~~0.29~~0.77 for the rain gauges and ~~0.23~~0.66 for the PERSIANN-CCS QPEs. The average relative error was ~~20~~-14% between the two precipitation products,~~.~~ ~~A~~and this relative error could be reasonably reduced by the post-process~~ed~~ing method presented in this paper.

2). The applicability of the Liuxihe model is prove~~d~~n by 30 accepted flood simulation results in the LKRB and 10 in the Beijiang catchment. ~~Especially~~In particular, the simulated results are quite good for the~~of~~ 10 karst flood events ~~are quite good~~ in the Beijiang catchment, where the karst is very developed. The average value of the Nash–Sutcliffe coefficient (C) is 0.92, the correlation coefficient (R) is 0.91, the process relative error (P) is 0.11, the peak flow relative error (E) is 0.08, the water balance coefficient (W) is 0.94, and the peak flow time error (T) is 3 hours~~, respectively~~.

The parameter~~s~~ sensitivity analysis for the Liuxihe model shows that the parameters –θsat, θs, θfc, Ks~~-~~, V, K, and χ are highly sensitive; z, b, Sw, Sp, n~~-~~, n1 and ω ~~are~~have medium– sensitivit~~y~~e~~,~~; and λ, Ep~~-~~, Cwl are insensitive parameters. ~~And t~~The sequence of parameters sensitivity is as follows: ~~S~~saturated water content~~/~~, θsat > ~~S~~saturation permeability coefficient~~/~~, θs > ~~F~~field capacity~~/~~, θfc > ~~S~~saturated hydraulic conductivity~~/~~, Ks > ~~M~~macro crack volume ratio~~/~~, V > Muskingum routing method (~~T~~the slope of the water storage content and flow curve)~~/~~, K> Muskingum routing method (the proportion of the flow)~~/~~, χ > ~~S~~soil layer thickness~~/~~, z > ~~S~~soil coefficient~~/~~, b > ~~B~~bottom width~~/~~, Sw > ~~B~~bottom slope~~/~~, Sp > ~~S~~slope roughness~~/~~, n > ~~C~~channel roughness~~/~~, n_1 > ~~D~~depletion coefficient ~~/~~, ω > ~~E~~evaporation coefficient~~/~~, λ> ~~P~~potential evaporation~~/~~, Ep > ~~W~~wilting percentage~~/~~, Cwl.

3~~2~~). ~~The average relative error is 20% between the two precipitation products was 20%. And this This relative error could be reduced reasonably reduced by the post-processed method presented in this paper.~~ The flood simulation results ~~with~~ from the post-processed PERSIANN-CCS QPEs are better than that ~~of~~ from the initial QPEs.~~,~~ ~~t~~The~~The~~ average values of the six evaluation indices, including the Nash–Sutcliffe coefficient (C), correlation coefficient (R), process relative error (P), peak flow relative error (E), water balance coefficient (W), and peak flow time error (T)~~—~~, with the initial— PERSIANN-CCS QPEs ~~are~~ were 0.66, 0.69, 0.28, 24%, 0.81 and ~~-32~~ -10 hours, respectively, while those ~~with~~ from the post-processed QPEs ~~are~~ were 0.73, 0.77, 0.22, 10%, 0.86 and ~~-25~~ -8 hours, respectively. ~~It~~This result ~~means~~ indicates that the method used in this study for ~~QPEs~~ post-process~~ed~~ing QPEs is effective~~,~~ and could improve the ~~effect of the~~ PERSIANN-CCS ~~QPEs~~QPE capability.

~~3~~4). The ~~coupling~~ coupled model parameters should be re-optimized using the post-processed PERSIANN-CCS QPEs. ~~Because it~~ This approach had~~has a~~ better performance in the flood simulation than that when the ~~same~~ model parameters were the same as those from the~~as~~ rain gauges. The average ~~value~~values of the Nash–Sutcliffe coefficient (C), correlation coefficient (R), process relative error (P), peak flow relative error (E), ~~,~~water balance coefficient (W), and peak flow time error (T)~~—~~ ~~with the same model parameters as rain gauge are~~ were 0.73, 0.77, 0.22, 10%, 0.86 and ~~-25~~ -8 hours, respectively, when the model parameters were the same as the rain gauge; however,~~but~~ those ~~with~~ obtained from the re-optimized model parameters ~~are~~ were 0.80, ~~0.83~~0.84, 0.20, 6%, ~~0.88~~0.89 and ~~—~~ ~~-7~~ -5 hours, respectively. ~~It~~ Thus, the proposed method significantly improves the model performance ~~significantly~~.

~~4~~5). The simulated karst ~~floods~~flood process based on the precipitation observed ~~by~~ at the rain gauges ~~is~~ was the best. ~~And~~ In addition, the flood simulation results ~~by~~ using the PERSIANN-CCS QPEs after post-~~processed~~ processing and re-~~optimized~~ optimizing the model parameters ~~could make the~~improved the coupled ~~coupling~~ model performance ~~much better~~. The average value of the Nash–Sutcliffe coefficient ~~has a~~ increased by 14% ~~increase~~, the correlation coefficient ~~has a~~increased by ~~14~~15% ~~increase~~, the process relative error ~~has a~~decreased by 8% ~~decrease~~, the peak flow relative error ~~has a~~decreased by 18% ~~decrease~~, the water balance coefficient ~~has a~~increased by ~~7~~8% ~~increase~~, and the peak flow time error ~~has~~ ~~had~~exhibited a ~~25~~5 ~~hours~~ -hour decrease~~, respectively~~. Among the~~m~~se parameters, the peak flow relative error ~~and the peak flow time error have the biggest improvement~~improved the most; thus, these parameters are the most important in terms of~~which are the greatest concerned factors in a~~ flood prediction in karst river basins.

Data availability

All ~~the~~ data used in this paper are available~~,~~ ~~and could be~~ findable, accessible, interoperable, and reusable (FAIR).

The rain gauge precipitation and river flow discharge data are provided by the Bureau of Hydrology, Pearl River Water Resources Commission, China, and are exclusively used for this study.

The PERSIANN QPEs data are provided by the Center for Hydrometeorology and Remote Sensing, Department of Civil and Environmental Engineering, University of California, Irvine~~. T~~. The PERSIANN-CCS QPEs real-time data in this paper ~~could~~ can be downloaded for free from http://hydis8.eng.uci.edu/CCS/.

The Liuxihe model used in this study is provided by Yangbo Chen, Department of Water Resources and

Environment, Sun Yat-~~sen~~Sen University, Guangzhou-, China.

Catchment property data for the Liuxihe model including the DEM, land-use and soil-type data can ~~could~~ be downloaded for free ~~in~~ from open-source databases. The DEM is downloaded from the shuttle radar topography mission database at http://srtm.csi.cgiar.org. The land use type data are~~is~~ downloaded from http: //landcover.usgs.gov, and the soil type data is downloaded from http://www.isric.org.

Competing interests~~.~~:

The authors declare that they have no conflicts of interest to disclose.

Acknowledgements. This s~~S~~tudy is supported by the Open Project Program of the Chongqing Key Laboratory of Karst Environment (Grant No. Cqk201801), ~~. T~~the Chongqing Municipal Science and Technology Commission Fellowship Fund (No. cstc2016jcyjys0003), and the National key research and development program of China (2016YFC0502306).

Edited by: Ji Li

Figures

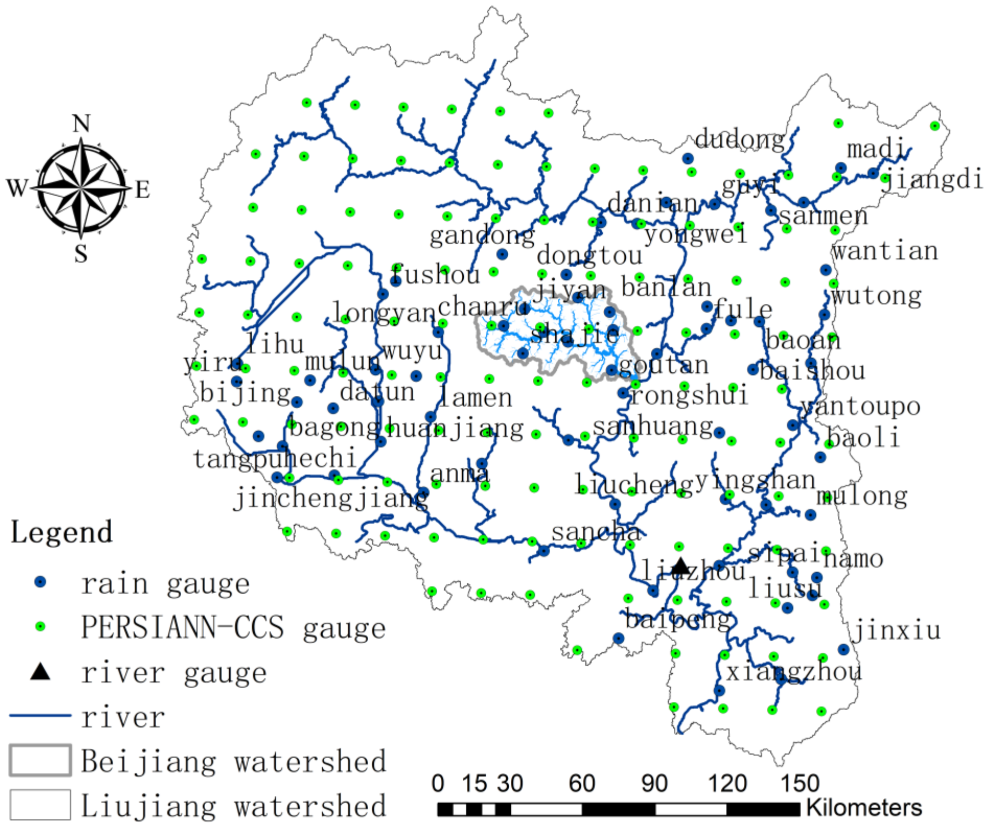

a. Sketch map of the Liujiang River Basin（LKRB）

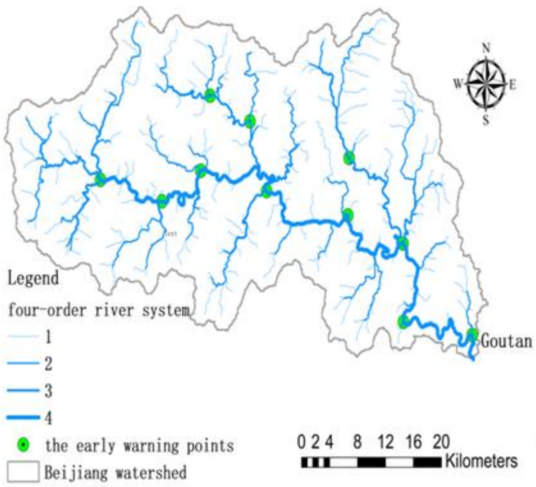

b. The early warning points

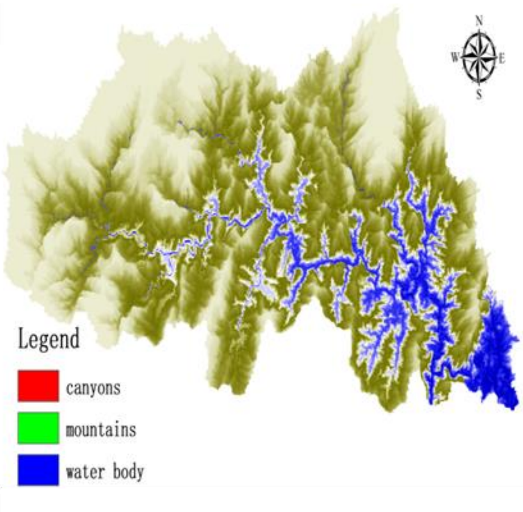

c. Three-dimensional topography

Figure –1. Sketch map of Liujiang and the Beijiang –catchment

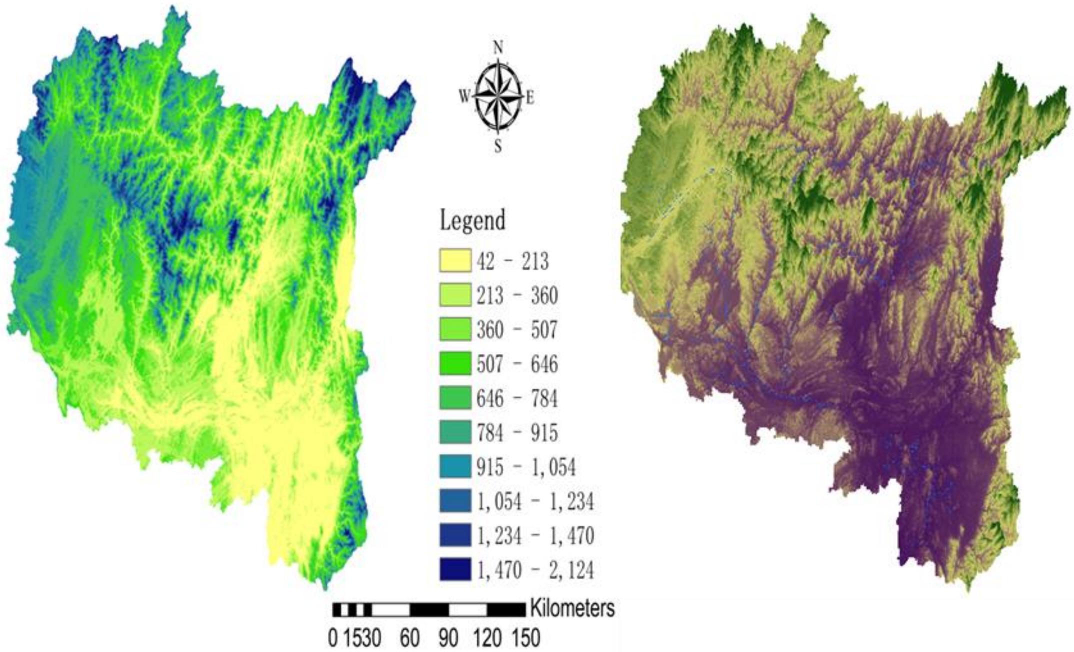

a. The DEM map b. Three-dimensional topographical map

Figure 2. The DEM and three-dimensional topographical map of the LKRB

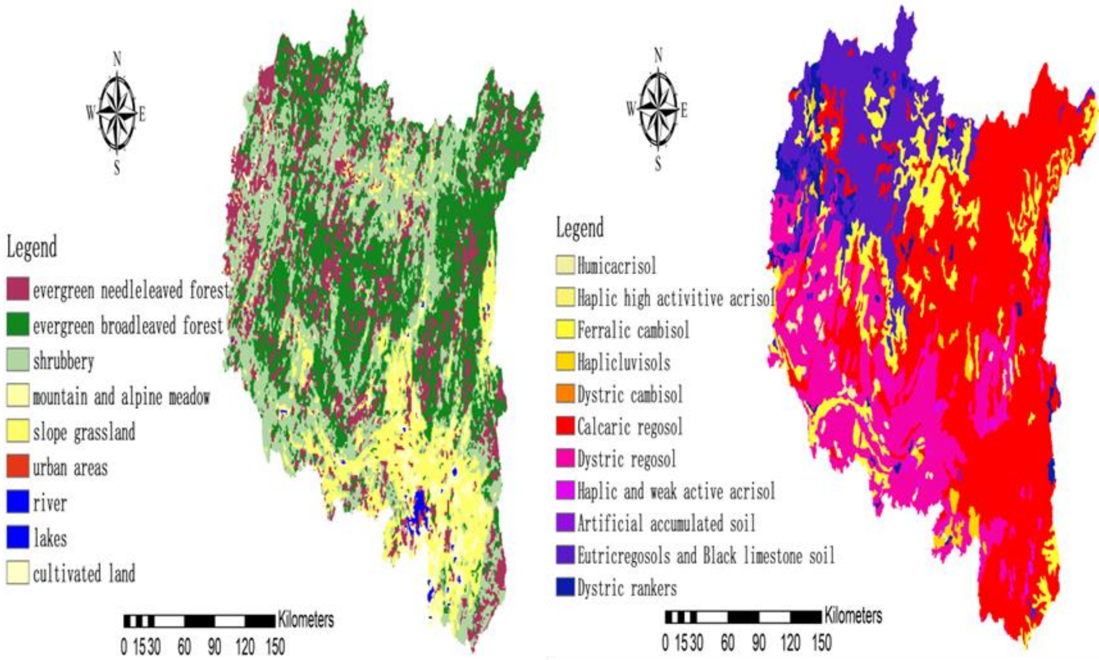

(a) land use types (b) soil types

Figure 3. The property data for the Liuxihe model in the LKRB

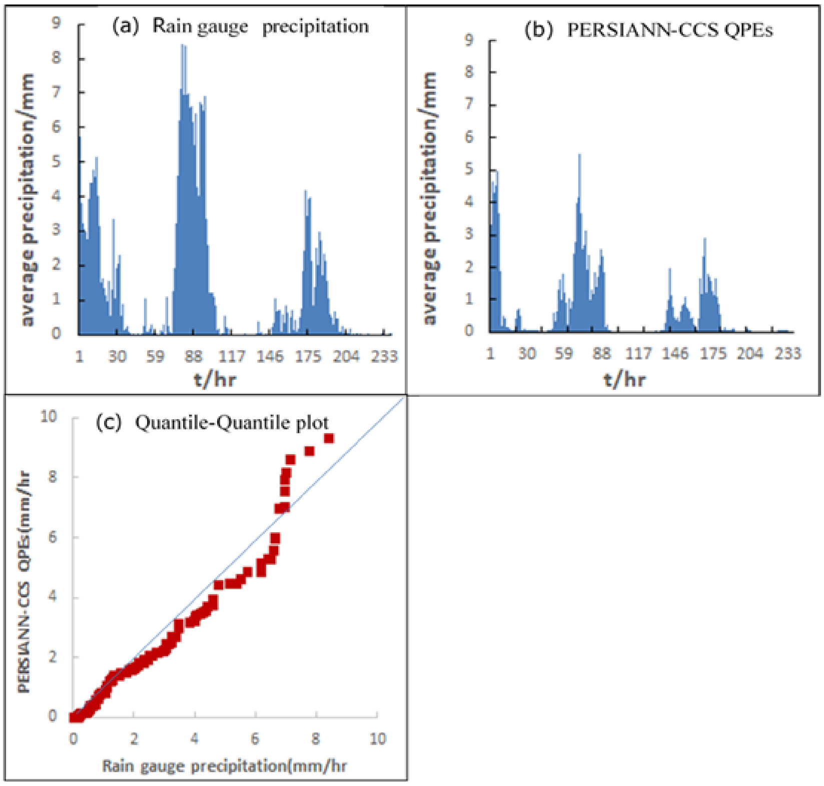

Figure 4. Precipitation pattern comparison of two precipitation products (2008)~~,~~: (a) is the average precipitation of rain gauges, (b) is the average precipitation of PERSIANN-CCS QPEs, and (c) is the ~~Q~~quantile-~~Q~~quantile plot, in which the 45-degree line is used to compare the two precipitation products.

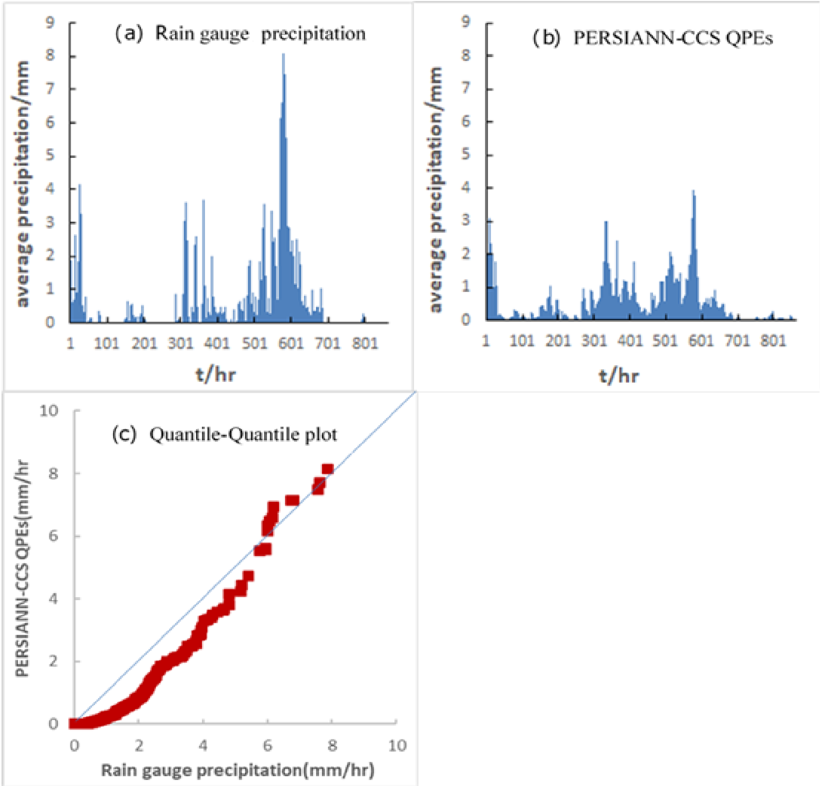

Figure 5. Precipitation pattern comparison of two precipitation products (2009): (a) is the average precipitation of rain gauges, (b) is the average precipitation of PERSIANN-CCS QPEs, and (c) is the quantile-quantile plot, in which the 45-degree line is used to compare the two precipitation products.

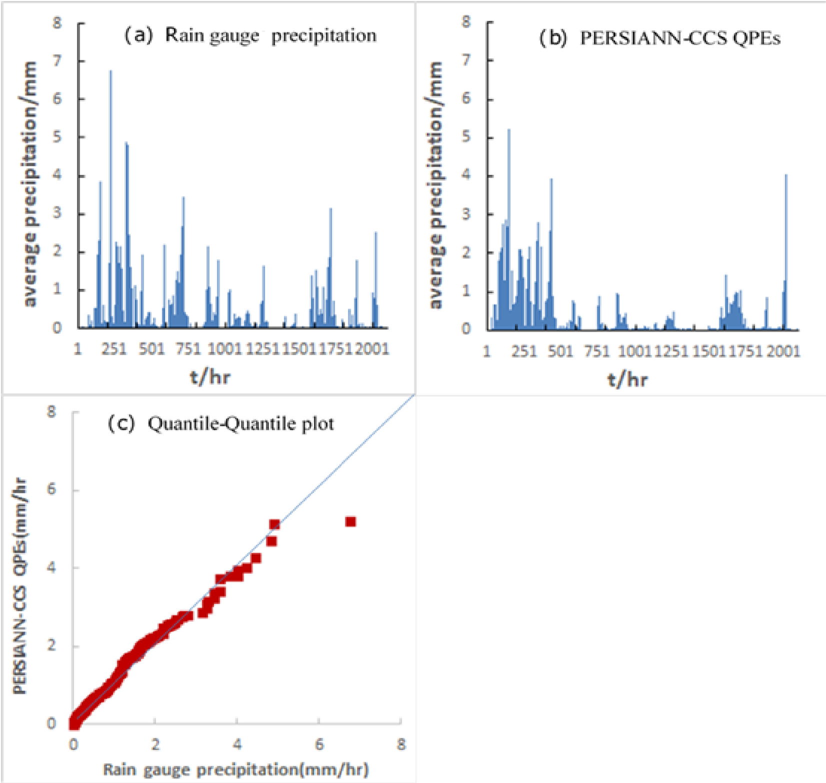

Figure 6. Precipitation pattern comparison of two precipitation products (2011): (a) is the average precipitation of rain gauges, (b) is the average precipitation of PERSIANN-CCS QPEs, and (c) is the quantile-quantile plot, in which the 45-degree line is used to compare the two precipitation products.

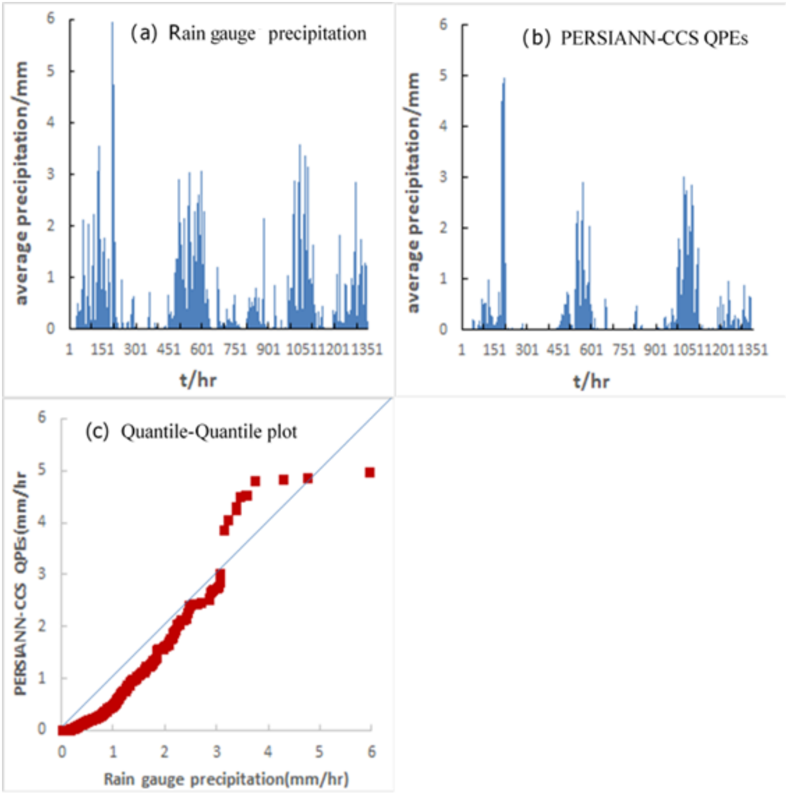

Figure 7. Precipitation pattern comparison of two precipitation products (2012): (a) is the average precipitation of rain gauges, (b) is the average precipitation of PERSIANN-CCS QPEs, and (c) is the quantile-quantile plot, in which the 45-degree line is used to compare the two precipitation products.

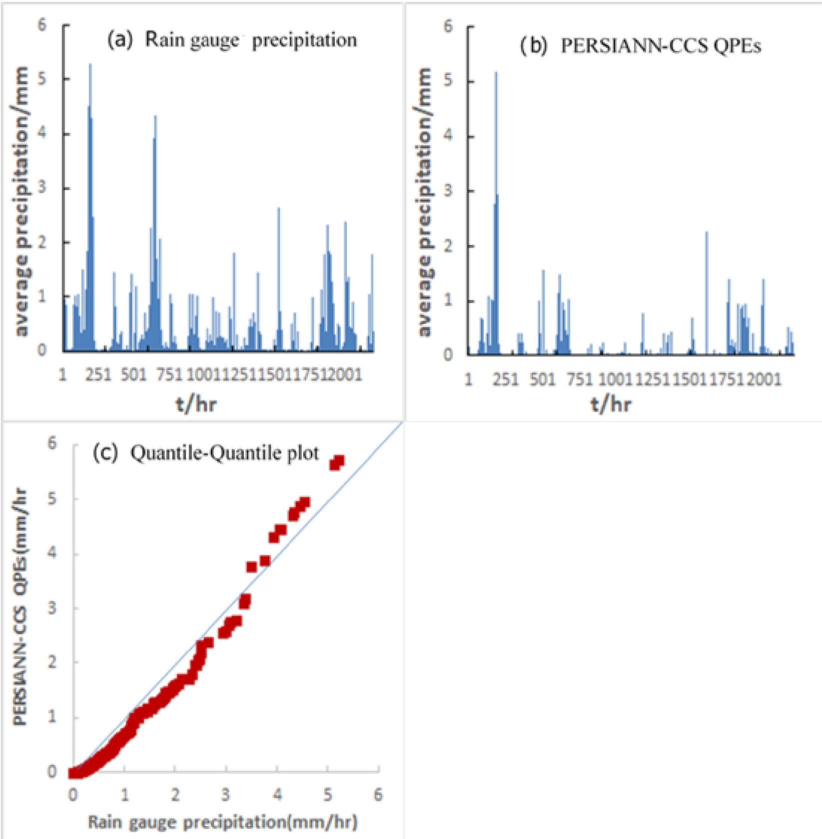

Figure 8. Precipitation pattern comparison of two precipitation products (2013): (a) is the average precipitation of rain gauges, (b) is the average precipitation of PERSIANN-CCS QPEs, and (c) is the quantile-quantile plot, in which the 45-degree line is used to compare the two precipitation products.

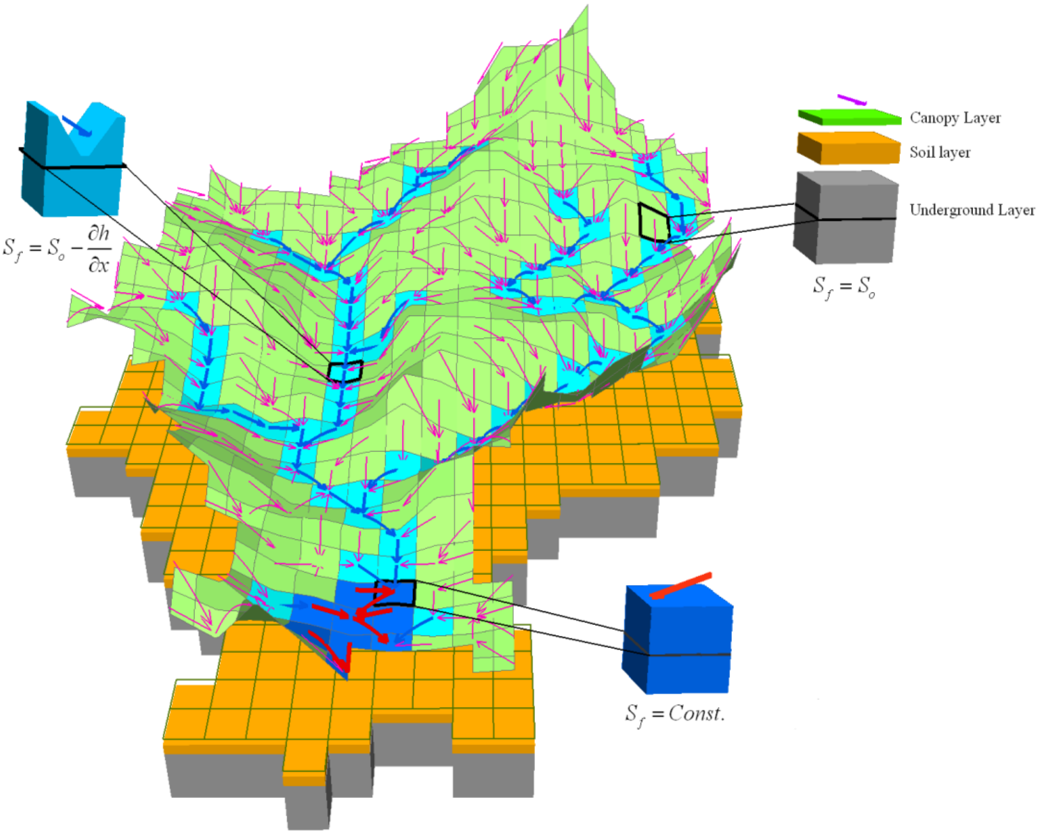

Figure 9. The structure of the Liuxihe model

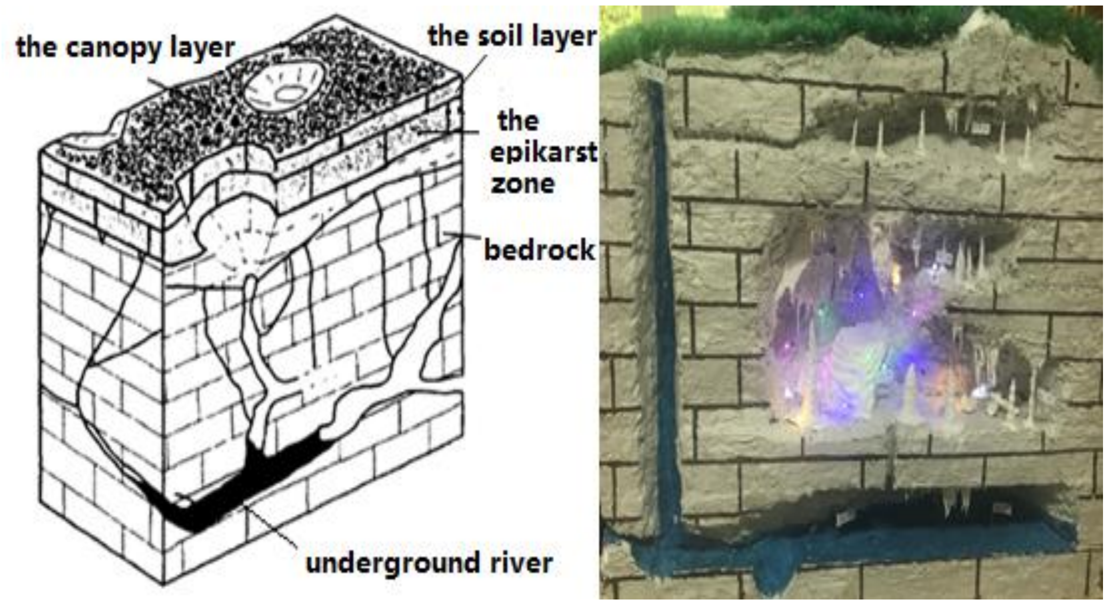

a. The structure of the KHRU (Ren, 2006~~)~~ b. ~~The~~ ~~P~~photograph of the three-dimensional ~~space~~ structure of the KHRU

Figure 10. Sketch map of the KHRU

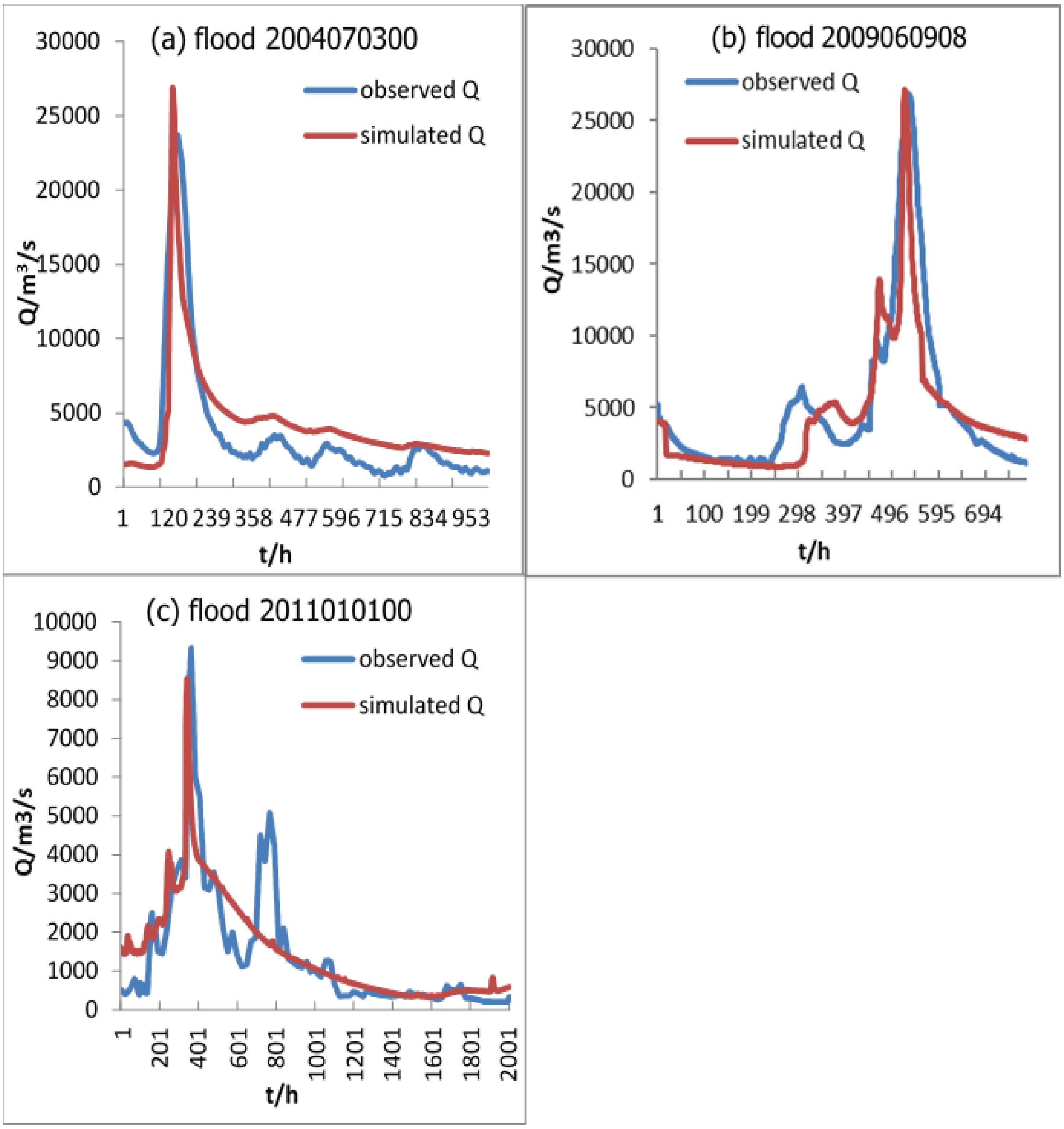

Figure 11. The flood simulation results obtained through parameter optimization by the improved PSO algorithm

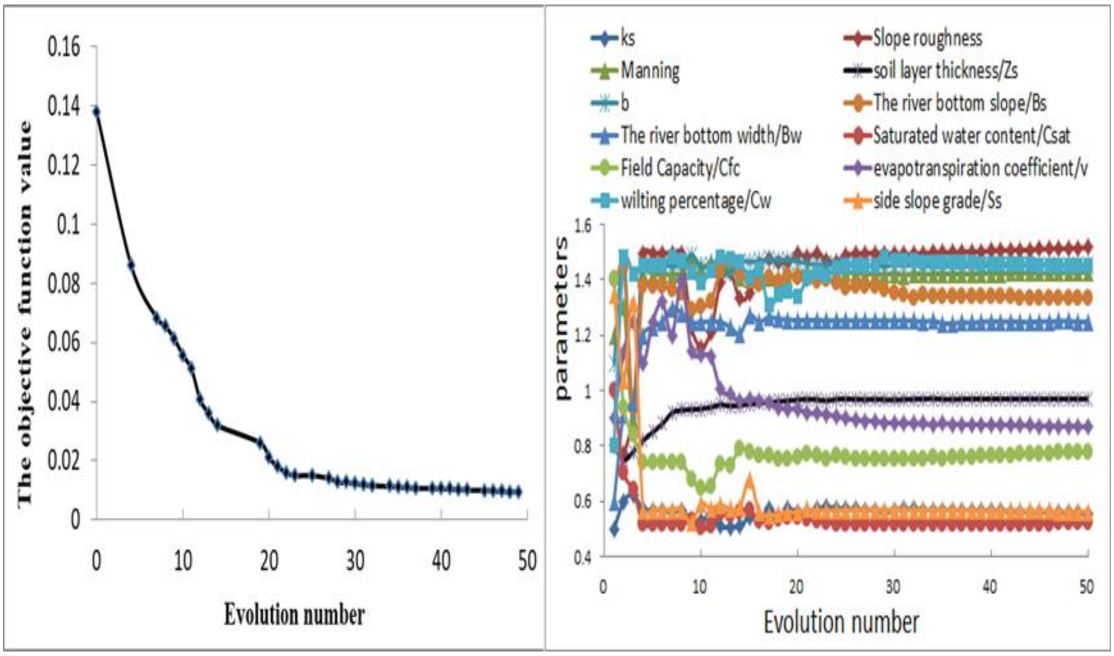

(a) The objective function evolution result (b) The parameter~~s~~ evolution result

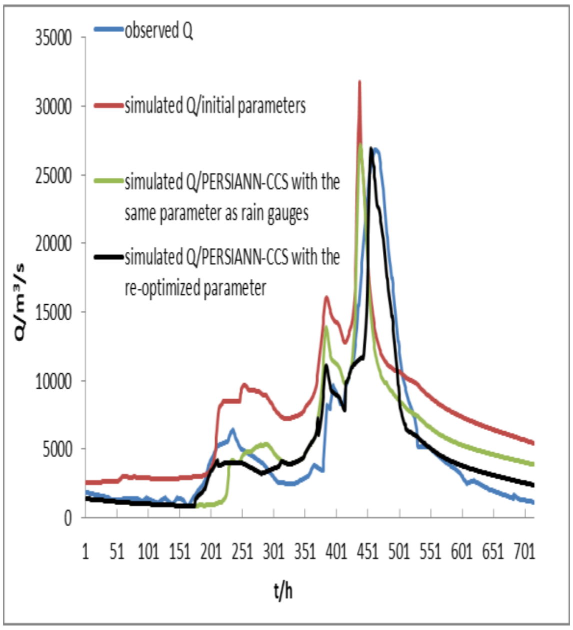

c) The simulated flood process ~~by~~ using the optimized model parameters

Figure 12. Parameter optimization results with the improved PSO algorithm

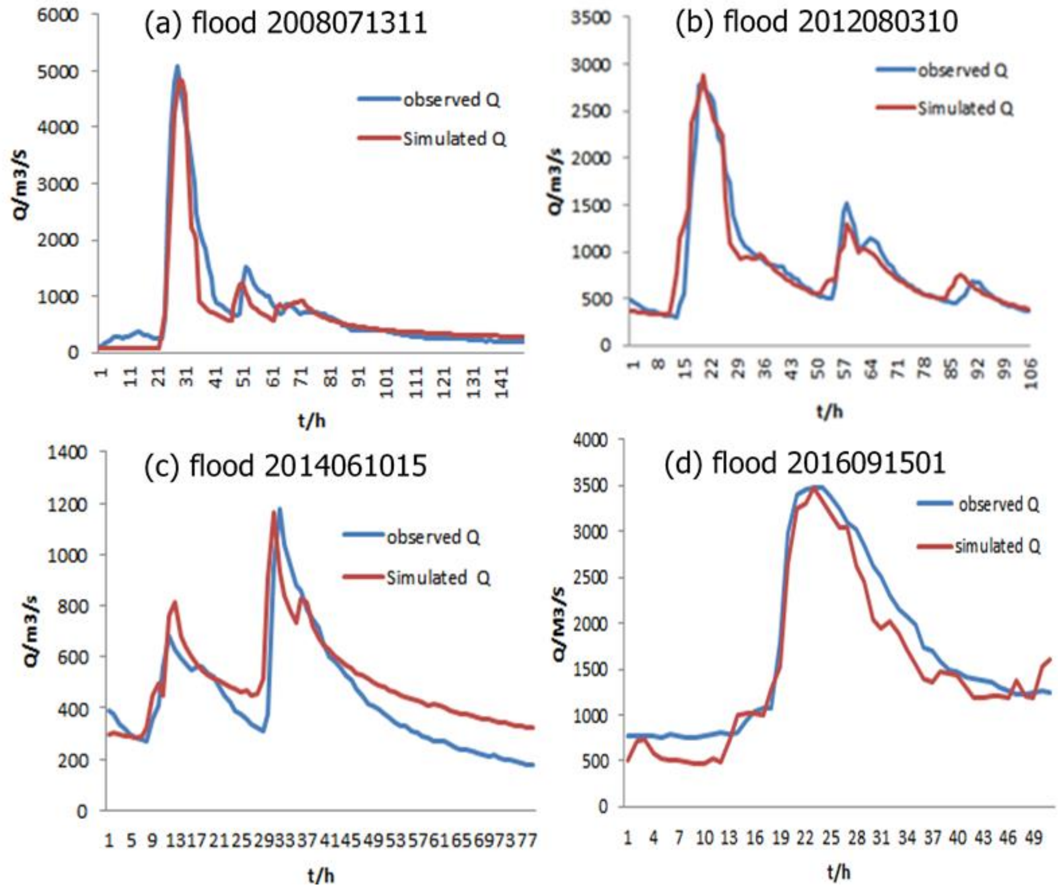

Figure 13. 4 karst flood simulation results ~~by~~ from the Liuxihe model in the Beijiang catchment

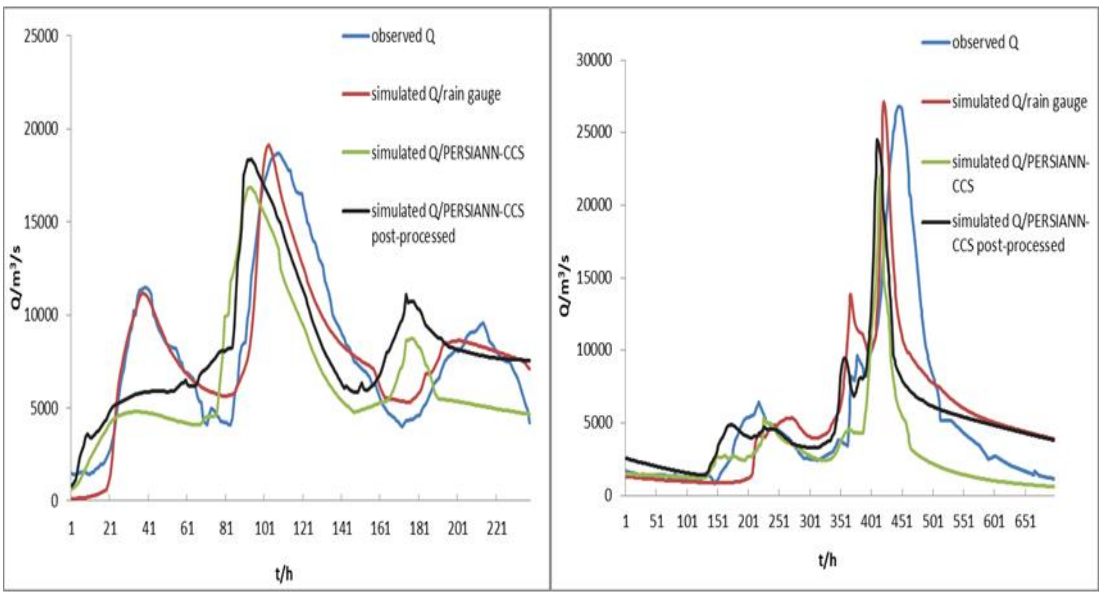

(a) ~~(a)f~~Flood event 200806090200 (b) ~~f~~Flood event 200906090800

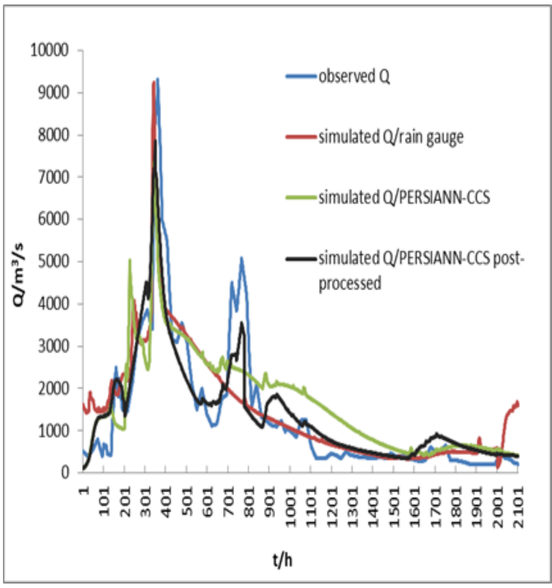

(c) ~~f~~Flood event 201106010900

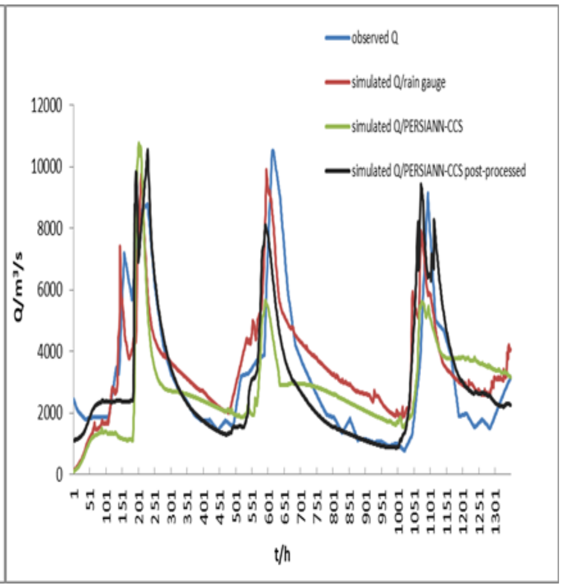

(d) ~~f~~Flood event 201206022000

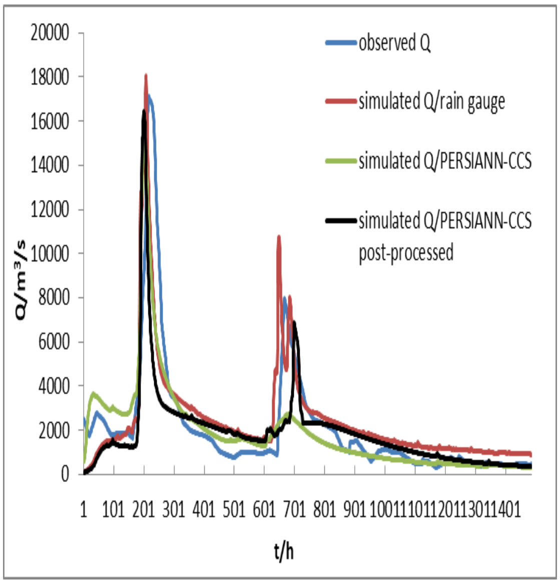

(e) ~~f~~Flood event 201306011400

Figure 14. The flood simulation results of the coupl~~ing~~ed model with the two precipitation products

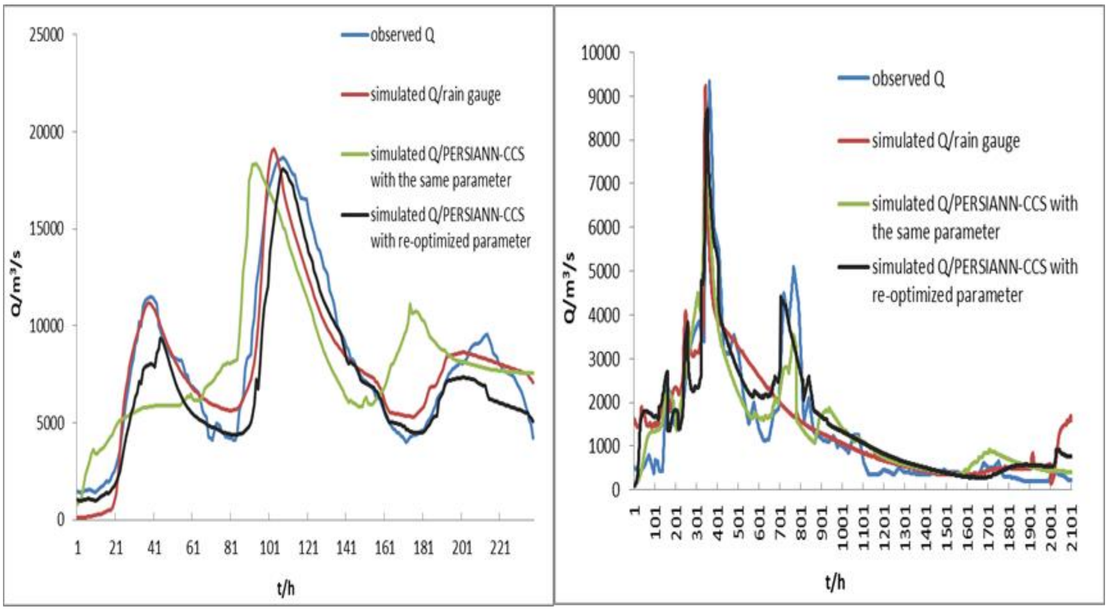

(a) ~~(a)~~F~~f~~lood event 200806090200 (b) ~~f~~Flood event 201106010900

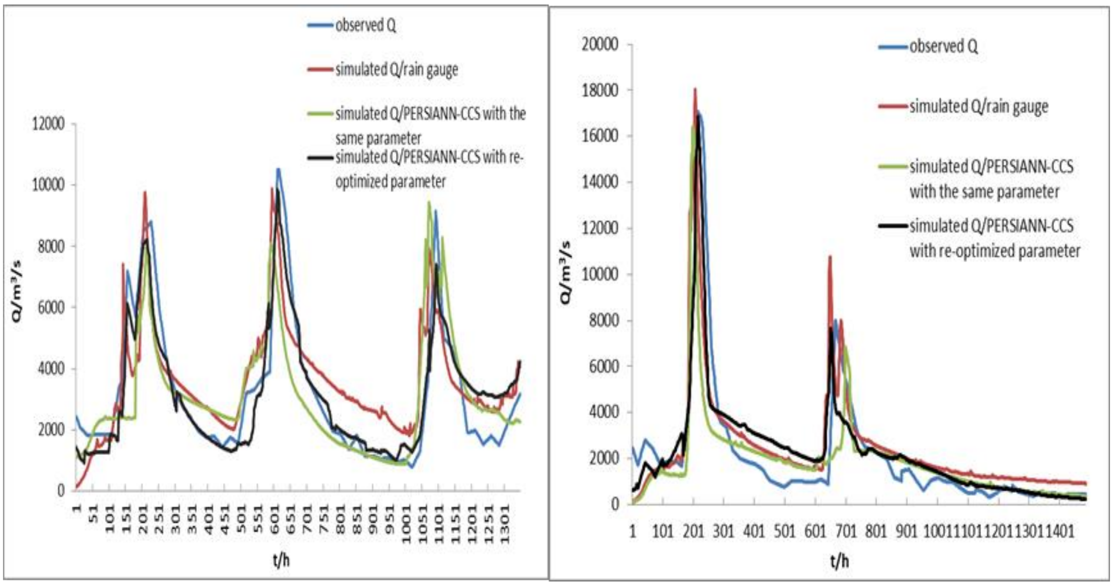

(c) ~~f~~Flood event 201206022000 (d) ~~f~~Flood event 201306011400

Figure 15. Coupled flood simulation results ~~with~~ using the same parameter as the rain gauge precipitation and using the re-optimized parameter ~~with~~ from the post-processed PERSIANN-CCS QPEs

Tables

Table 1. Precipitation pattern comparison of the two precipitation products

~~flood~~Floods	~~t~~Type	~~a~~Average precipitation (mm)	~~r~~Relative bias %
200806090200	rain gauge	1.37 ~~0.37~~	—
	PERSIANN-CCS QPEs	1.22 ~~0.31~~	-11 ~~-16~~
200906090800	rain gauge	0.74 ~~0.24~~	—
	PERSIANN-CCS QPEs	0.62 ~~0.18~~	-16 ~~-25~~
201106010900	rain gauge	0.42 ~~0.22~~	—
	PERSIANN-CCS QPEs	0.39 ~~0.19~~	-7 ~~-14~~
201206022000	rain gauge	0.78 ~~0.38~~	—
	PERSIANN-CCS QPEs	0.63 ~~0.30~~	-19 ~~-21~~
201306011400	rain gauge	0.53 ~~0.22~~	—
	PERSIANN-CCS QPEs	0.43 ~~0.17~~	-20 ~~-23~~
average value	rain gauge	0.77 ~~0.29~~	—
	PERSIANN-CCS QPEs	0.66 ~~0.23~~	-14 ~~-20~~

Table 2. The parameters of the model

(a) The parameters of the coupling model

Parameters types	Name	Variable name	Physical property	Sensitivity	Adjustability
Evapotranspiration	Potential evaporation	E_p	Meteorology	insensitive	adjustable
	Evaporation coefficient	λ	Vegetation type	medium sensitive	adjustable
	Wilting percentage	C_{wl}	Vegetation type	insensitive	adjustable
The epikarst zone	Thickness	h	Soil type& Karst rock property	sensitive	unadjustable
	Saturated water content	θ_{sat}	Soil type	highly sensitive	adjustable
	Saturation permeability coefficient	θ_s	Soil type	highly sensitive	adjustable
	Macro crack volume ratio	V	Karst rock property	highly sensitive	adjustable
	Field capacity	θ_{fc}	Soil type	sensitive	adjustable
Rainfall-runoff	Soil layer thickness	z	Soil type	sensitive	adjustable
	Saturated hydraulic	K_s	Soil type	highly	adjustable

	conductivity			sensitive	
	Soil coefficient	b	Soil type	sensitive	adjustable
	Flow direction	F_d	Landform	highly sensitive	unadjustable
	Slope	S_0	Landform	highly sensitive	unadjustable
	Bottom slope	S_p	Landform	sensitive	adjustable
	Bottom width	S_w	Landform	sensitive	adjustable
	Slope roughness	n	Landform &Vegetation type	sensitive	adjustable
	Channel roughness	n_1	Landform &Vegetation type	sensitive	adjustable
The underground river	Depletion coefficient	ω	Landform &Soil type	medium sensitive	adjustable
	Muskingum routing method / The slope of the water storage content and flow curve	K	Landform	highly sensitive	adjustable
	Muskingum routing method/the proportion of the flow	χ	Landform	highly sensitive	adjustable

(b) The physical parameters of the epikarst zone

Thickness/ h (m)	Saturated water content/θsat (g/cm^3)	Saturation permeability coefficient/θs (mm/hr)	Macro crack volume ratio/V (m^3/m^3)	Field capacity/θfc (mm)
3-10	0.12-0.3	100-420	0.05-0.15	0.16-0.3

(c)The rainfall infiltration coefficient of different karst landforms

Landforms	karst strongly developed	karst moderately developed	karst poorly developed
closed depression	0.6-0.8	0.4-0.6	0.15-0.18
not closed depression	0.4-0.7	0.3-0.5	0.18-0.2
monadnock, platform	0.2-0.3	0.2-0.3	0.2-0.25
gully, slope	0.01-0.2	0.01-0.2	0.01-0.2

Table 3. The evaluation indices of flood simulation results obtained through parameter optimization by the improved PSO algorithm

~~F~~floods	Nash–Sutcliffe-~~Sutcliffe~~ coefficient/C	Correlation coefficient/R	Process relative error/P%	Peak flow relative error/E%	The coefficient of water balance/W	Peak time error/T(h)
2004070300	0.78	0.82	0.23	0.08	0.85	-8
2009060908	0.95	0.92	0.17	0.04	0.09	-5
2011010100	0.8	0.84	0.26	0.03	1.02	-7

Table 4. The calculation results of the parameters sensitivity in the Liuxihe model

Floods	Potential evaporation/Ep	Evaporation coefficient/λ	Wilting percentage/Cwl	Saturated water content/θsat	Saturation permeability coefficient/θs	Macro crack volume ratio/V	Field capacity/θfc	Soil layer thickness/z	Saturated hydraulic conductivity/Ks
200407030000	0.06	0.08	0.02	0.92	0.90	0.77	0.85	0.68	0.82
	Soil coefficient/b	Bottom slope/Sp	Bottom width/Sw	Slope roughness/n	Channel roughness/n1	Depletion coefficient/ω	Muskingum routing method / The slope of the water storage content and flow curve/K	Muskingum routing method /the proportion of the flow/χ	
	0.65	0.36	0.49	0.27	0.19	0.12	0.76	0.75	
200906090800	Potential evaporation/Ep	Evaporation coefficient/λ	Wilting percentage/Cwl	Saturated water content/θsat	Saturation permeability coefficient/θs	Macro crack volume ratio/V	Field capacity/θfc	Soil layer thickness/z	Saturated hydraulic conductivity/Ks
	0.08	0.11	0.05	0.96	0.92	0.81	0.89	0.65	0.87

	Soil coefficient/b	Bottom slope/Sp	Bottom width/Sw	Slope roughness/n	Channel roughness/n_1	Depletion coefficient/ω	Muskingum routing method/ The slope of the water storage content and flow curve/K	Muskingum routing method/the proportion of the flow/χ	
	0.62	0.54	0.58	0.32	0.25	0.12	0.78	0.78	
2011060 10900	Potential evaporation/Ep	Evaporation coefficient/λ	Wilting percentage/Cwl	Saturated water content/θsat	Saturation permeability coefficient/θs	Macro crack volume ratio/V	Field capacity/θfc	Soil layer thickness/z	Saturated hydraulic conductivity/Ks
	0.12	0.25	0.07	0.89	0.82	0.71	0.79	0.62	0.75
	Soil coefficient/b	Bottom slope/Sp	Bottom width/Sw	Slope roughness/n	Channel roughness/n_1	Depletion coefficient/ω	Muskingum routing method/ The slope of the water storage content and flow curve/K	Muskingum routing method/the proportion of the flow/χ	
	0.58	0.52	0.55	0.48	0.42	0.33	0.72	0.68	

Table 5. The evaluation indices of the simulated flood results based on the Liuxihe model in the LKRB

F~~f~~loods	Nash–Sutcliffe- ~~Sutcliffe~~ coefficient/C	Correlation coefficient/R	Process relative error/P%	Peak flow relative error/E%	The coefficient of water balance/W	Peak time error/T (h)
1982081219	0.84	0.75	0.3	0.01	0.83	-4
1983020308	0.82	0.84	0.21	0.04	0.89	-5
1984010100	0.75	0.89	0.26	0.14	0.96	-3
1985010100	0.73	0.87	0.17	0.01	1.05	-5
1986010100	0.83	0.85	0.23	0.04	0.94	4
1987050100	0.93	0.76	0.1	0.05	1.01	-6
1988051620	0.84	0.8	0.15	0.04	0.9	-8
1989042600	0.64	0.74	0.39	0.02	0.88	-5
1990050100	0.85	0.87	0.14	0.03	0.85	-3
1991053118	0.8	0.76	0.25	0.04	0.95	10
1992042900	0.66	0.84	0.2	0.11	0.89	5
1993060900	0.91	0.89	0.24	0.09	1.05	-8
1994060700	0.93	0.85	0.14	0.04	0.85	-6
1995052100	0.82	0.7	0.2	0.01	0.81	-10
1996060600	0.9	0.93	0.18	0.02	0.86	-5
1997060400	0.84	0.87	0.13	0.06	0.95	-4
1998051600	0.83	0.85	0.3	0.01	1.05	-6
1999061700	0.6	0.83	0.15	0.05	0.8	-5
2000052100	0.79	0.89	0.26	0.06	0.83	-8
2001051500	0.8	0.82	0.25	0.07	0.82	-6
2002042600	0.86	0.9	0.24	0.02	0.87	-2
2003060600	0.92	0.85	0.14	0.04	0.76	-4
2004070300	0.78	0.82	0.23	0.08	0.85	-8
2005061400	0.76	0.76	0.35	0.06	0.74	-5
2006060400	0.82	0.83	0.3	0.1	0.86	-3
2008060900	0.8	0.91	0.15	0.03	0.89	-6
2009060908	0.95	0.92	0.17	0.04	0.09	-5
2011010100	0.8	0.84	0.26	0.03	1.02	-7
2012010100	0.82	0.79	0.2	0.05	0.8	-6
2013010100	0.95	0.82	0.2	0.06	0.92	-4
mean value	0.82	0.83	0.22	0.05	0.87	-6

Table 6. The evaluation indices of the simulated flood results based on the Liuxihe model in the Beijiang catchment

Floods	Nash–Sutcliffe-~~Sutcliffe~~ coefficient/C	Correlation coefficient/R	Process relative error/P%	Peak flow relative error/E%	The coefficient of water balance/W	Peak flow time error/T (h)
2000101512	0.89	0.92	0.11	0.09	0.93	-3
2003091014	0.91	0.88	0.13	0.11	0.89	-2
2005070815	0.93	0.89	0.09	0.13	0.95	2
2008071311	0.97	0.89	0.08	0.09	0.95	-1
2010081012	0.87	0.93	0.12	0.07	0.91	-4
2012080310	0.9	0.95	0.06	0.05	0.96	2
2013091210	0.92	0.91	0.09	0.09	0.89	3
2014061015	0.93	0.93	0.18	0.07	1.08	-2
2015091008	0.93	0.89	0.13	0.08	0.92	-3
2016091501	0.94	0.9	0.11	0.04	0.92	1
mean value	0.92	0.91	0.11	0.08	0.94	3

Table 7. Evaluation indices of simulated flood events ~~with~~ using the initial PERSIANN-CCS QPEs and the post-processed ~~ones~~values

~~flood~~Floods	~~t~~Type	Nash–Sutcliffe-~~Sutcliffe~~ coefficient/C	Correlation coefficient/R	Process relative error/P%	Peak flow relative error/E%	The coefficient of water balance/W	Peak time error/T (h)
200806090000	rain gauge	0.8	0.91	15	3	0.89	-6
	PERSIANN-CCS QPEs	0.6	0.65	26	36	0.83	-10
	the post-processed PERSIANN-CCS QPEs	0.63	0.73	21	6	0.92	-8
200906090800	rain gauge	0.95	0.92	17	4	0.9	-12
	PERSIANN-CCS QPEs	0.67	0.61	28	34	0.79	-16
	the post-processed PERSIANN-CCS QPEs	0.75	0.64	22	14	0.85	-13
2011060	rain gauge	0.8	0.84	16	3	1.02	-7

10900	PERSIANN-CCS QPEs	0.65	0.83	25	21	0.89	-10
	the post-processed PERSIANN-CCS QPEs	0.75	0.85	21	12	0.92	-8
20120602200	rain gauge	0.82	0.79	20	5	0.8	-6
	PERSIANN-CCS QPEs	0.69	0.54	31	17	0.75	-9
	the post-processed PERSIANN-CCS QPEs	0.71	0.74	23	12	0.78	-7
201306011400	rain gauge	0.95	0.82	20	6	0.92	-4
	PERSIANN-CCS QPEs	0.7	0.84	28	10	0.79	-7
	the post-processed PERSIANN-CCS QPEs	0.82	0.89	24	7	0.85	-5
average value	rain gauge	0.86	0.86	18	4	0.91	-7
	PERSIANN-CCS QPEs	0.66	0.69	28	24	0.81	-10
	the post-processed PERSIANN-CCS QPEs	0.73	0.77	22	10	0.86	-8

Table 8. The effect of recalibrating the coupling model parameters

~~flood~~Floods	Parameter type	Nash–Sutcliffe-~~Sutcliffe~~ coefficient/C	Correlation coefficient/R	Process relative error/P %	Peak flow relative error/E %	The coefficient of water balance/W	Peak flow time error/T (h)
200806090000	Coupling model/the same model parameters as rain gauges	0.63	0.73	21	6	0.92	-10
	Coupling model/re-optimized model parameters	0.76	0.83	18	5	0.93	-4
201106010900	Coupling model/the same model parameters as rain gauges	0.75	0.85	21	12	0.92	-8
	Coupling model/re-optimized model parameters	0.78	0.87	19	6	0.94	-6
20120602200	Coupling model/the same model parameters as rain gauges	0.71	0.74	23	12	0.78	-7
	Coupling model/re-optimized model parameters	0.78	0.76	21	8	0.79	-4
201306011400	Coupling model/the same model parameters as rain gauges	0.82	0.89	24	7	0.85	-5

	Coupling model/re-optimized model parameters	0.86	0.91	22	6	0.87	-4
average value	Coupling model/the same model parameters as rain gauges	0.73	0.77	22	10	0.86	-8
	Coupling model/re-optimized model parameters	0.80	0.84	20	6	0.89	-5

References

Abbott, M. B., Bathurst, J. C., Cunge, J. A., O'Connell, P. E.,and Rasmussen, J.: An Introduction to the European HydrologicSystem-System Hydrologue Europeen, 'SHE', a: History and Philosophy of a Physically-based, Distributed Modelling System,J. Hydrol., 87, 45–59, 1986a.

Abbott, M. B.,Bathurst, J. C.,Cunge, J. A., O'Connell, P. E., and Rasmussen, J.: An Introduction to the European Hydrologic System-System Hydrologue Europeen, 'SHE', b: Structure of a Physically based, distributed modeling System, J. Hydrol., 87,61–77, 1986b.

Ahilan, S., O'Sullivan, J. J., and Bruen, M.: Influences on flood frequency distribution in Irish catchments. 34th IAHR World Congress 2011: Balance and Uncertainty: Water in a Changing World. International Assn for Hydro-Environment Engineering and Research, 2012.

Ambroise, B., Beven, K., and Freer, J.: Toward a generalization of the TOPMODEL concepts: Topographic indices of hydrologic similarity, Water Resour. Res., 32,2135–2145, 1996.

Ashouri, H., Hsu, K.L., Sorooshi,S., Braithwaite, D. K., Knapp, K. R., and Cecil, L. D.: PERSIANN-CDR: Daily Precipitation Climate Data Record from Multisatellite Observations for Hydrological and Climate Studies. Bulletin of the American Meteorological Society, 96(1):197-210, 2014.

Atkinson, T.C.: Diffuse flow and conduit flow in limestone terrain in the Mendip Hills, Somerset (Great Britain). Journal of Hydrology, 35(1-2):93-110, 1977.

Bartsotas, N., Nikolopoulos, E., Anagnostou, E., and Kallos, G.: Improving satellite quantitative precipitation estimates through the use of high-resolution numerical weather predictions: Similarities and contrasts between the Alps and Blue Nile region// EGU General Assembly Conference. EGU General Assembly Conference Abstracts, 2017.

Birk,S., Geyer, T., Liedl, R., and Sauter, M.: Process-based interpretation of tracer tests in carbonate aquifers. Ground Water, 43(3): 381-388, 2005.

Chen, Y.B.: Liuxihe Model, China Science and Technology Press, Peking, China, September 2009.

Chen, Y.B., Li, J., and Xu, H.J.: Improving flood prediction capability of physically based distributed hydrological models by parameter optimization, Hydrol. Earth Syst. Sci., 20, 375–392, doi:10.5194/hess-20-375-2016, 2016.

Chen, Y.B., Li, J., Wang, H., Qin, J., and Dong, L.: Large-watershed flood prediction with high-resolution distributed hydrological model, Hydrol. Earth Syst. Sci., 21, 735–749, doi:10.5194/hess-21-735-2017, 2017.

Choi, J., Harvey, J. W., and Conklin, M. H.: Use of multi-parameter sensitivity analysis to determine relative importance of factors influencing natural attenuation of mining contaminants. the Toxic Substances Hydrology Program Meeting, Charleston ,south Carolina: 1999 .

Davis W.M.: Relation of geography to geology. Geological Society of America Bulletin, 23,1912.

Delrieu,G., Bonnifait, L., Kirstetter, P. E., and Boudevillain, B.: Dependence of radar quantitative precipitation estimation error on the rain intensity in the Cévennes region, France. Hydrological Sciences Journal, 59(7):1308-1319,2014.

Doummar, J., Margane, A., Sauter, M., and Geyer, T.: Assessment of transport parameters in a karst system under various flow periods through extensive analysis of artificial tracer tests// EGU General Assembly Conference. EGU General Assembly Conference Abstracts, 2012.

Duan, J.,and Miller,N.L.: A generalized power function for the subsurface transmissivity profile in TOPMODEL. Water Resources Research, 33(11):2559–2562, 1997.

Falorni, G., Teles, V., Vivoni, E. R., Bras, R. L., and Amaratunga, K. S.: Analysis and characterization of the vertical accuracy of digital elevation models from the Shuttle RadarTopography Mission, J. Geophys. Res.-Earth, 110, F02005, doi:10.1029/2003JF000113, 2005.

Fan, K.K.,Duan, L.M.,Zhang, Q., Shi, P.J., Liu, J.Y., Gu, X.H., and Kong, D.D.: Downscaling Analysis of TRMM Precipitation Based on Multiple High-resolution Satellite Data in the Inner Mongolia, China. Scientia Geographica Sinica, 37(9):1411-1421, 2017.

Faure, D., Gaussiat, N., Tabary, P., and Urban, B.: Real time integration of foreign radar quantitative precipitation estimations (QPEs) in the French national QPE mosaic// Conference on Radar Meteorology, AMS,21-21, 2015.

Ford, D., and Williams P.W.: Karst Geomorphology and Hydrology. Geographical Journal, 157(1):87,1991.

Freeze, R. A. and Harlan, R. L.: Blueprint for a physically-based,digitally simulated, hydrologic response model, J. Hydrology., 9,237–258, 1969.

Goldscheider, N., and Drew, D.: Methods in Karst Hydrogeology: IAH:International Contributions to Hydrogeology, 26. CRC Press, 2007.

Goudenhoofdt E, Delobbe L.: Evaluation of radar-gauge merging methods for quantitative precipitation estimates. Hydrology & Earth System Sciences, 13(2):195-203.,2009.

Hartmann, A., Barberá, J. A., Lange, J., Andreo, B., and Weiler, M.: Progress in the hydrologic simulation of time variant recharge areas of karst systems – Exemplified at a karst spring in Southern Spain. Advances in Water Resources, 54(2):149-160, 2013.

He, R.X.: Impact of Aquatic Bacteria on Karst Carbon Sequestration: A Case Study in the Honghua

Hydropower Station, Liujiang Bsin. Southwest University,2017.

Hirpa, F. A., Gebremichael, M., and Hopson, T.: Evaluation of high-resolution satellite precipitation products over very complex terrain in ethiopia. J.appl.meteor.climatol, 49(5), 1044-1051.,2010.

Hsu, K. L., Gupta, H. V., Gao, X.G, and Soroosh,S.: Estimation of physical variables from multichannel remotely sensed imagery using a neural network: Application to rainfall estimation. Water Resources Research, 35(5):1605-1618,1999.

Hsu, K.L, Yang,H., and Soroosh,S.: Rainfall Estimation Using a Cloud Patch Classification Map// Measuring Precipitation From Space. Springer Netherlands,329-342, 2007.

Hussain, Y., Satgé, F., Hussain, M. B., Martinez-Carvajal, H., Bonnet, M. P., and Cárdenas-Soto, M.: Performance of CMORPH, TMPA, and PERSIANN rainfall datasets over plain, mountainous, and glacial regions of Pakistan. Theoretical & Applied Climatology, 131(3-4), 1119-1132,2018.

Hu, Q.F., Yang,D.W.,Wang,Y.T.,Yang,H.B.,and Liu,Y.: Characteristics and sources of errors in daily T R MM precipitation product over Ganjiang River basin in China . ADVANCES IN WATER SCIENCE,24(6)：794-800,2013.

Kovacs,A., and Perrochet,P.: Hydrograph Analysis for Parameter Estimation of Connected and Karst Systems// Engineers Australia, 2011.

Li, J., Chen, Y.B., Wang, H.Y., Qin, J.M., Li, J., and Chiao, S.: Extending flood prediction lead time in a large watershed by coupling WRF QPF with a distributed hydrological model. Hydrology & Earth System Sciences Discussions, 21:1-45,2017.

Li,B.G.,and Tao,S.: Several Problems and Their Solutions in Surface Runoff Modeling. Bulletin of Soil and W ter Conservation, 20(3):47-49,2000.

Li,G.F.: Karst Hydrogeologic Characteristics and Water Resources in Guangxi,China, Carsologica Sinica,3:253-258,1996.

Li,X.M., and Ren,B.: The calculation method of non-closure small watershed of the mine water runoff in ungauged basins. Mineral Engineering Research, 2009.

Liu,H.M.Deng,H.P.,Sun,S.F.,and Xiao,Y.: .Numerically Test of Influence of Incorporation of TOPMODEL into Land Surface Model SSiB on Hydrological Simulation at Basin Scale.PLATEAU METEOROLOGY, 32(3):829-838,2013.

Liu, X.Y.,Yang, T., Hsu ,K.L., Liu, C., and Soroosh,S.: Evaluating the streamflow simulation capability of PERSIANN-CDR daily rainfall products in two river basins on the Tibetan Plateau. Hydrology & Earth System Sciences Discussions, 21(1):1-31, 2017.

Loveland, T. R., Merchant, J. W., Ohlen, D. O., and Brown, J. F.: Development of a Land Cover Characteristics Data Base for the Conterminous U.S., Photogram, Photogramm. Eng. Rem. S., 57, 1453–1463, 1991.

Loveland, T. R., Reed, B. C., Brown, J. F., Ohlen, D. O., Zhu, J., Yang, L., and Merchant, J. W.: Development of a Global Land Cover Characteristics Database and IGBP DISCover from 1-km AVHRR Data, Int. J. Remote Sens., 21, 1303–1330, 2000.

Moradkhani, and Meskele, T.T.: Satellite Rainfall Applications for Surface Hydrology. Springer Netherlands, 2010.

Neitsch,S.L.,J.G.Arnold,J.R.Kiniry and J.R.Williams.: Soi1 and Water Assessment Tool

Theoretical Documentation Version,2000.

Quinlan, J.F and Ewers, R.O.: Ground water flow in limestone terranes -strategy, rationale and procedure for reliable, efficient monitoring of ground water in karst areas. Mendeley, 8:167-173, 1985.

Quinlan, J. F., Davies, G. J., Jones, S. W., and Huntoon, P. W.: The applicability of numerical models to adequately characterize ground-water flow in karstic and other triple-porosity aquifers. 1288:114-133, 2011.

Rafieei,N.A., Norouzi,, A., Kim, B., and Seo, D.: J Fusion of multiple radar-based quantitative precipitation estimates (QPE) for high-resolution flash flood prediction in large urban areas// AGU Fall Meeting. AGU Fall Meeting Abstracts, 2014.

Ren,Q.W.: Water Quantity Evaluation Methodology Based on Modified SWAT Hydrological Modeling in Southwest Karst Area. China University of Geoscience, Wuhan ,China, 2006.

Romill, T. G. and Gebremichael, M.: Evaluation of satellite rainfall estimates over Ethiopian river basins. Hydrol. Earth Syst. Sci., 15, 1505–1514, 2011, doi:10.5194/hess-15-1505-2011.

Servat, E .,and Sakho,M.: Modelling and management of sustainable basin-scale water resource systems : proceedings of an international symposium held at Boulder, Proceedings of IAHS Symposium 6, IAHS Publication No.231,1995.

Sharma, A. and Tiwari, K. N.: A comparative appraisal of hydrological behavior of SRTM DEM at catchment level, J. Hydrol., 519, 1394–1404, 2014.

Shuster, E .T, and White,W.B.: Seasonal fluctuations in the chemistry of lime-stone springs: A possible means for characterizing carbonate aquifers. Journal of Hydrology, 14(2):93-128,1971.

Soroosh,S., Hsu ,K.L.,Gao,,X.G.,Hoshin,V.G.,Bisher,I.,and Braithwaite, D.: Evaluation of PERSIANN System Satellite-Based Estimates of Tropical Rainfall. Bulletin of the American Meteorological Society,81,2035-2046,2000.

Stenz, R.D.: Improving satellite quantitative precipitation estimates by incorporating deep convective cloud optical depth. Dissertations & Theses - Gradworks, 2014.

Tan ,M.L., and Santo,H.: Comparison of GPM IMERG, TMPA 3B42 and PERSIANN-CDR satellite precipitation products over Malaysia. Atmospheric Research, , 202, 2018.

Wardhana A, Pawitan H, and Dasanto B D.: Application of hourly radar-gauge merging method for quantitative precipitation estimates//012033,2017.

Williams,P.W.: Geomorohic inheritance and the development of tower karst Earth surface Progresses and landform.12,453-465,1987.

Yang,H., Hsu, K. L., Soroosh,S., and Gao, X.G.: Precipitation Estimation from Remotely Sensed Imagery Using an Artificial Neural Network Cloud Classification System. Journal of Applied Meteorology, 36(9):1176-1190,2004.

Yang,H.,Gochis, D., Cheng, J. T., Hsu, K. L., and Soroosh,S.: Evaluation of PERSIANN-CCS Rainfall Measurement Using the NAME Event Rain Gauge Network. Journal of Hydrometeorology, 8(3):469, 2007.

Zhang,C.,Jiang,Y.J.,Lian,Y.Q.,Yuan,D.X.,Pei,J.G.,and Jiang,G.H.: Rainfall-runoff simulation of a typical karst fengcong depression system using SWMM model-A case study of the Yaji experimental site in Guilin.Hydrogeology and Engineering Geology,34(3):10-14, 2007.